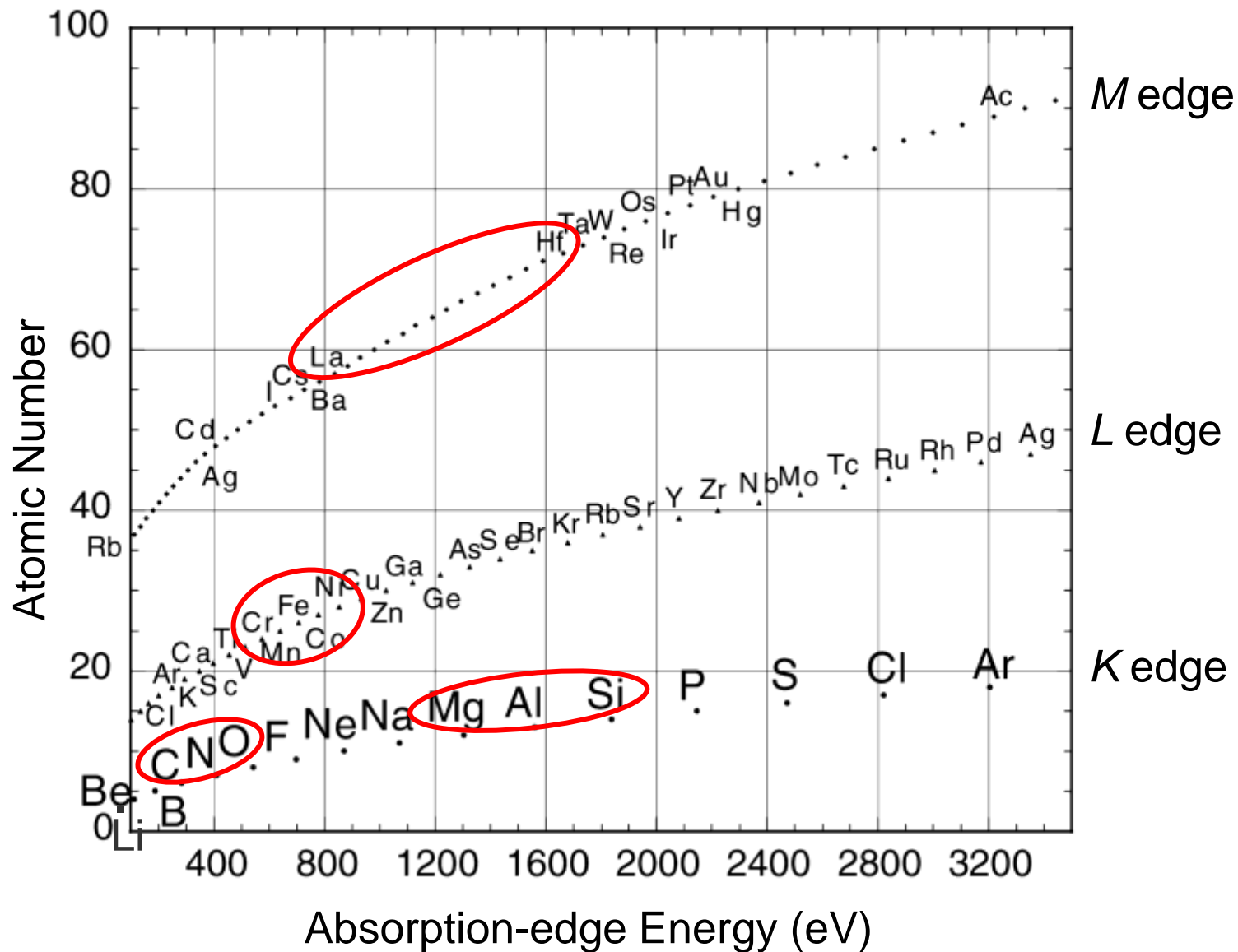


Soft X-ray Absorption Spectroscopy

Kenta Amemiya (KEK-PF)

Absorption Edges in the Soft X-ray Region



Studies using Soft X-ray

Soft X-ray Beamlines

~15/50 at Photon Factory (2.5 & 6.5 GeV)

~5/55 at Spring-8 (8 GeV)

Experimental Techniques

X-ray Absorption Spectroscopy (XAS)

Photoemission Spectroscopy (PES)

Resonant X-ray Scattering (RXS)

Applications:

Organic Molecules & Polymers (C, N, O...)

Magnetic Materials (Fe, Co, Ni, ...)

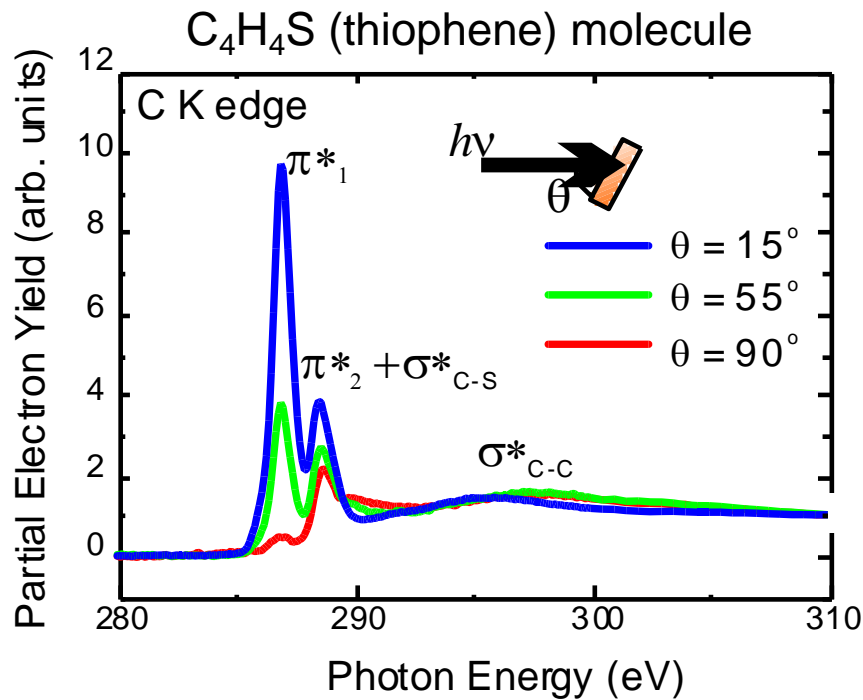
Surface & Thin Film

Soft X-ray Absorption Spectroscopy

1. Advantages and Disadvantages of Soft X-ray Absorption Spectroscopy (SXAS)
2. SXAS studies on Surface and Thin films
3. Novel SXAS Techniques
 - 3-1. Depth-resolved XAS
 - 3-2. Wavelength-dispersive XAS

X-ray Absorption Spectroscopy (XAS)

- Transition from core to unoccupied states -



1. Element selectivity

← Core-hole excitation (1s, 2p...)

(C: 290 eV, O: 530 eV, Fe: 710 eV, Ni: 850 eV...)

2. Information on chemical species

← Characteristic spectral features (π^* , σ^* ...)

3. Structural information (bond length, etc.)

EXAFS (Extended X-ray Absorption Fine Structure)

4. Information on anisotropy

← Linear polarization

(molecular orientation, lattice anisotropy)

5. Magnetic information

← Circular polarization

In the Soft X-ray region,

1. Vacuum environment is normally required. (**NOT ultra-high vacuum**)

Special sample cell is available for **ambient pressure**.

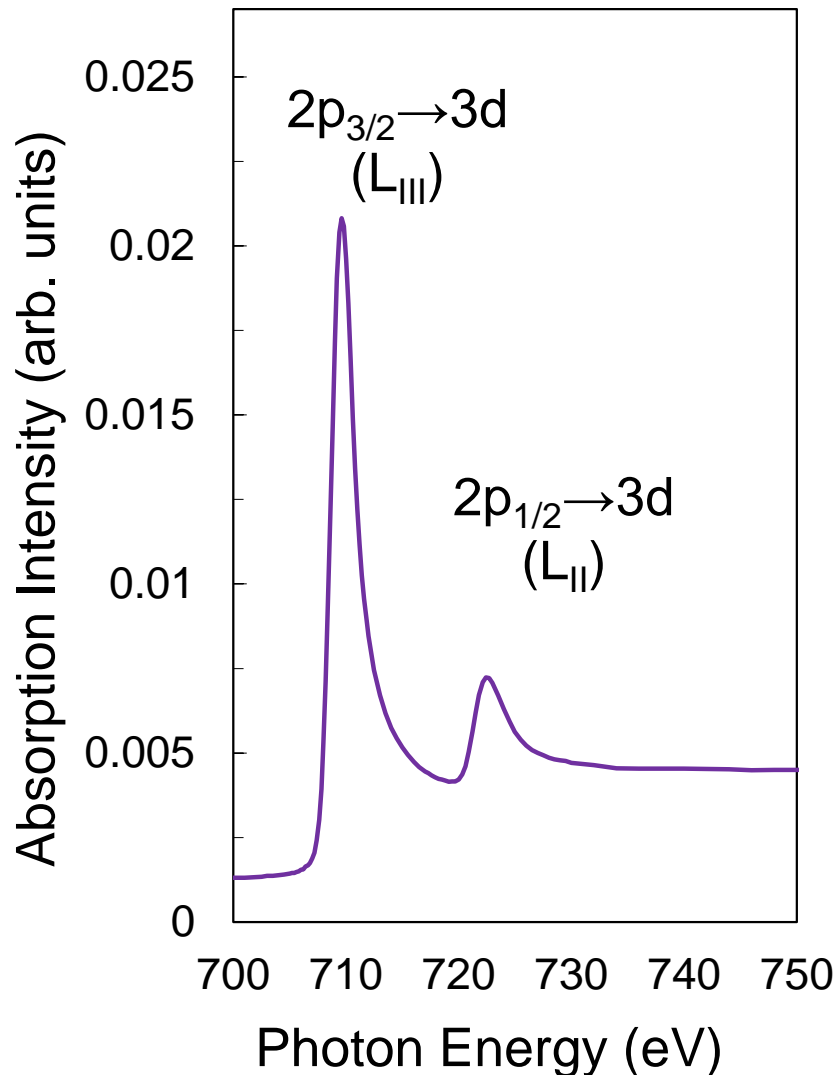
2. Surface sensitive

λ (probing depth):

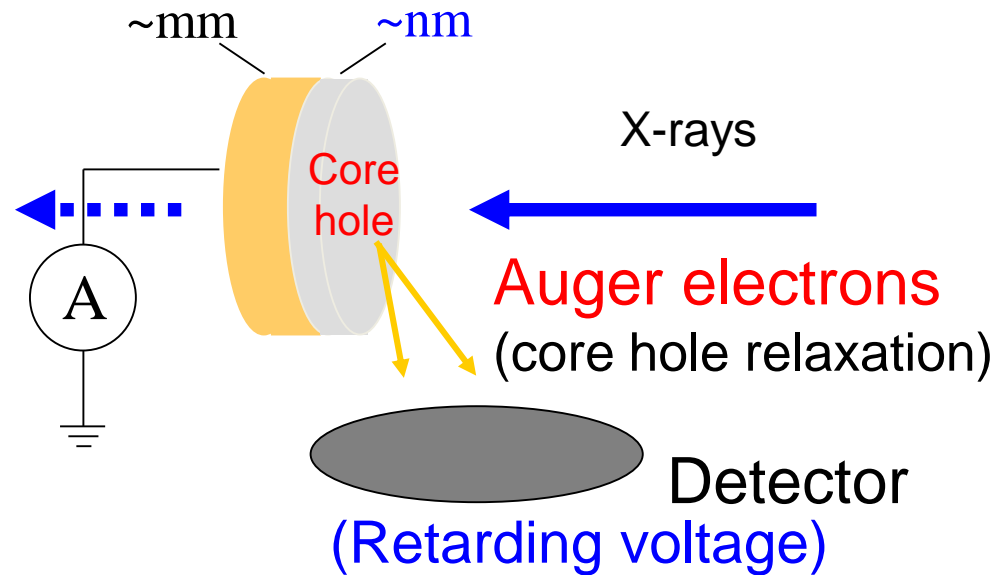
several nm for electron yield, $\sim 0.1 \mu\text{m}$ for fluorescence yield

XAS Measurement in the Soft X-ray Region

3 ML Fe / Cu(100) Fe L-edge XAS



How can we measure X-ray absorption spectrum ?



Electron yield XAS

Total electron yield (TEY) $\lambda \sim 3 \text{ nm}$

Partial electron yield (PEY) $\lambda \sim 1-2 \text{ nm}$

cf. Fluorescence yield (FY) $\lambda \sim 100 \text{ nm}$

Advantages and Disadvantages of SXAS

Short Penetration Length

- ☹️ Transmission mode can be available only for a very thin sample on a very thin or without substrate.
 - 😊 Electron yield mode is usually adopted because of high efficiency.
 - ☹️ Special care is necessary for insulators (powders might be OK).
 - ☹️ Fluorescence yield efficiency is very small for light elements.
<1 % for C, N, O
Be careful for the self absorption (saturation) effect.
- ☹️ Samples should be usually kept in vacuum (NOT ultra-high vacuum).
 - 😊 Some attempts have been made to realize ambient-pressure or liquid-state measurements.

Surface Sensitive

- 😊 Sub-monolayer samples can be investigated.
- ☹️ Bulk information is hardly obtained, especially in the electron yield mode.

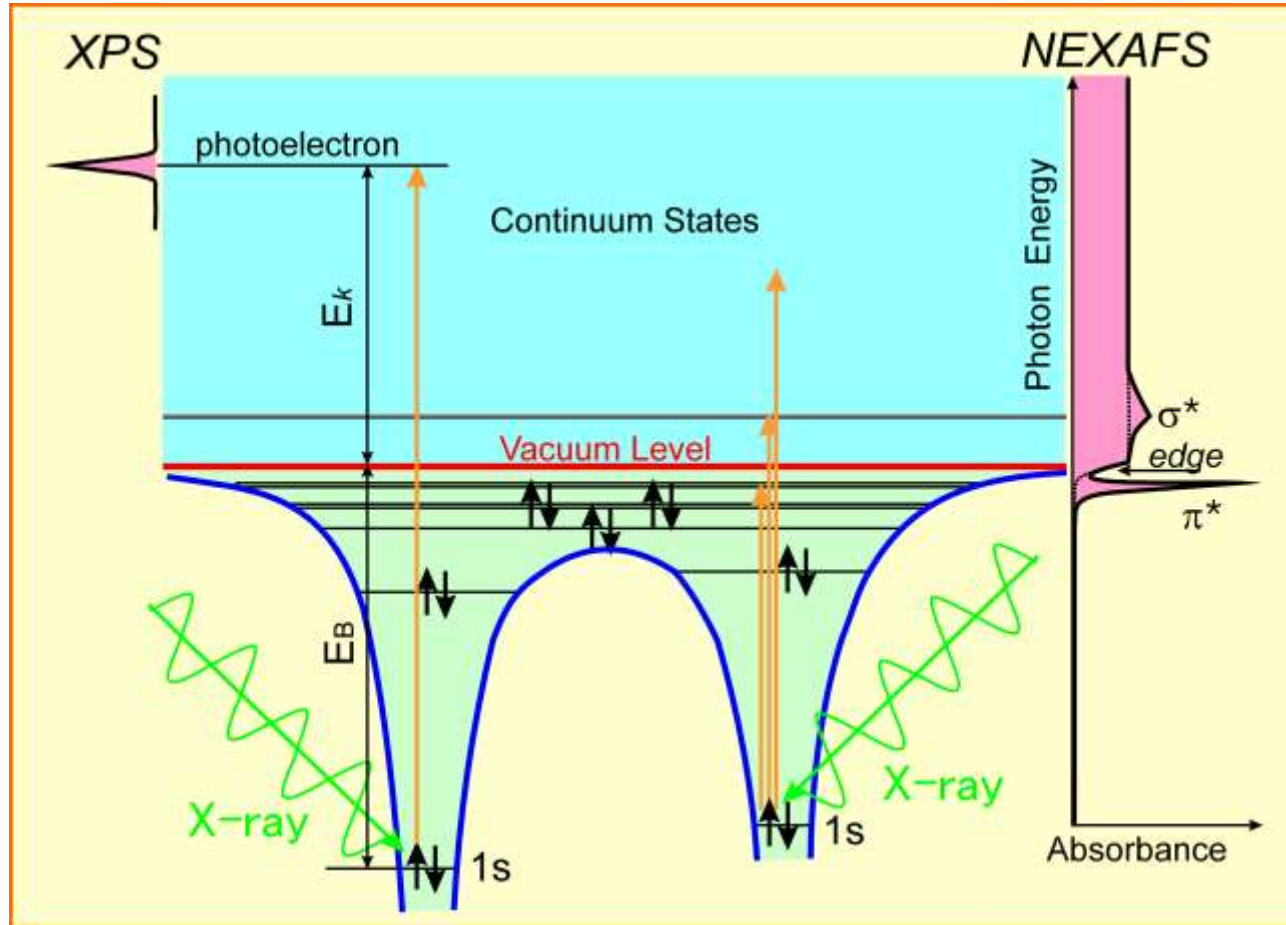
Sensitive to Electronic and Magnetic States of light elements

- 😊 Valence electrons can be directly investigated by $1s \rightarrow 2p$ excitation of C, N, O,... and $2p \rightarrow 3d$ excitation of 3d transition metals.

1. Advantages and Disadvantages of
Soft X-ray Absorption Spectroscopy (SXAS)
2. SXAS studies on Surface and Thin films
3. Novel SXAS Techniques
 - 3-1. Depth-resolved XAS
 - 3-2. Wavelength-dispersive XAS

Near-edge Spectroscopy

Near-edge X-ray Absorption Fine Structure (NEXAFS)
X-ray Absorption Near-edge Structure (XANES)



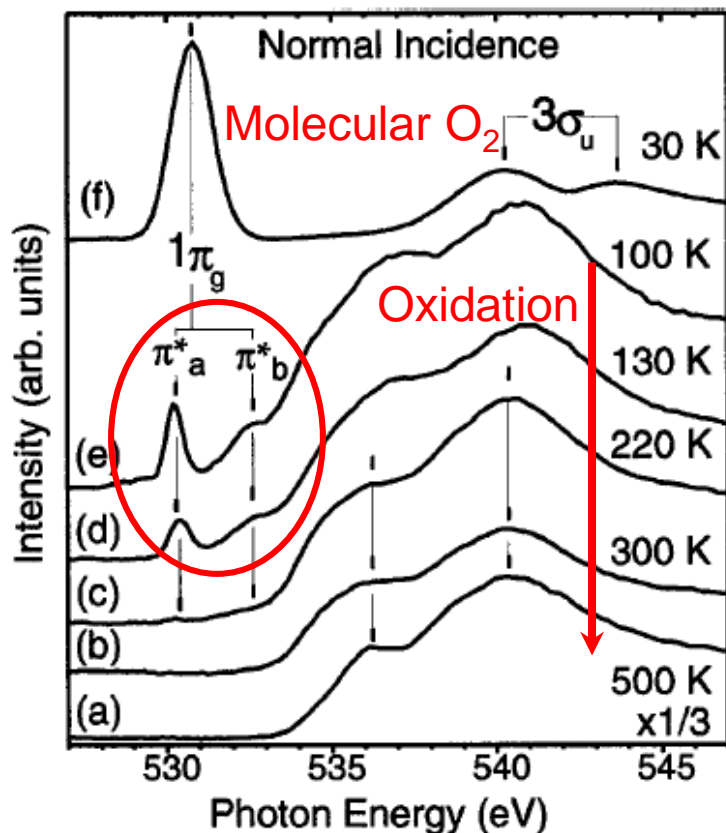
Chemical species

Structural information (orientation)

Near-edge Spectroscopy

Determination of Chemical Species

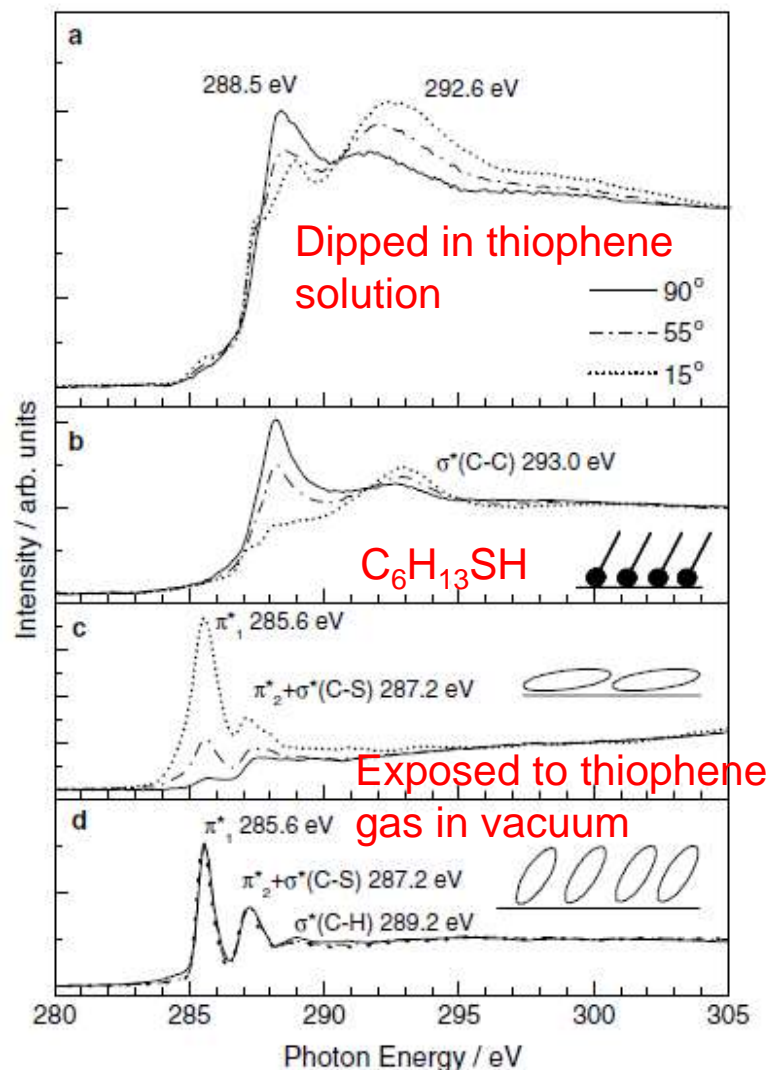
Initial oxidation process of Si



Existence of **molecular oxygen** in the initial stage of Si oxidation

Matsui et al., Phys. Rev. Lett. **85**, (2000) 630.

Thiophene (C₄H₄S) molecule on Au(111)

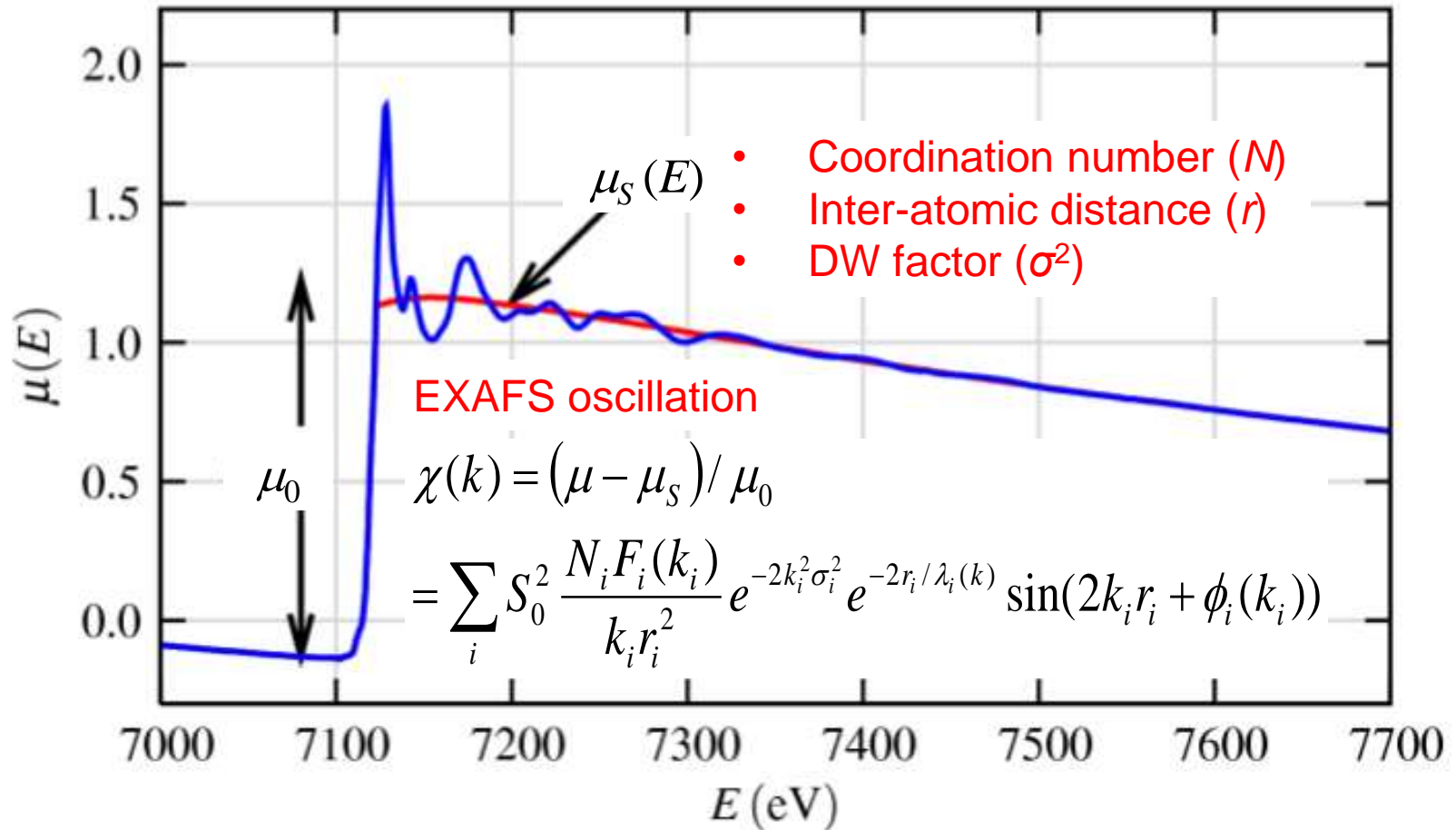


Different chemical species depending on preparation processes

Sako et al., Chem. Phys. Lett. **413**, (2005) 267.

Determination of Geometric Structure

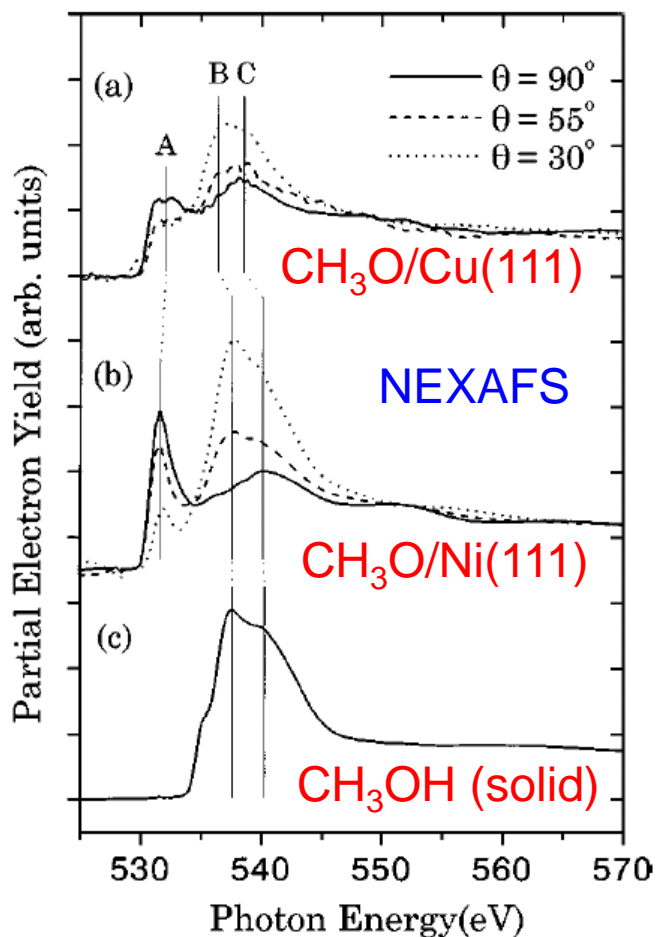
Extended X-ray Absorption Fine Structure (EXAFS)



Fe K -edge XAFS spectrum $\mu(E)$ of FeO

Determination of Geometric Structure

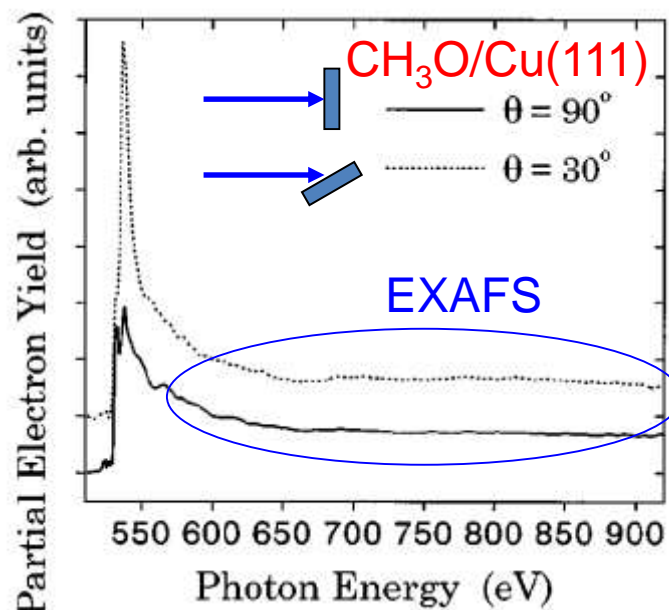
Amemiya et al., Phys. Rev. B **59**, (1999) 2307.



Peak B ($1s \rightarrow \sigma_{\text{CO}}^*$) -> **C-O bond length**
 Higher energy -> **Shorter bond**

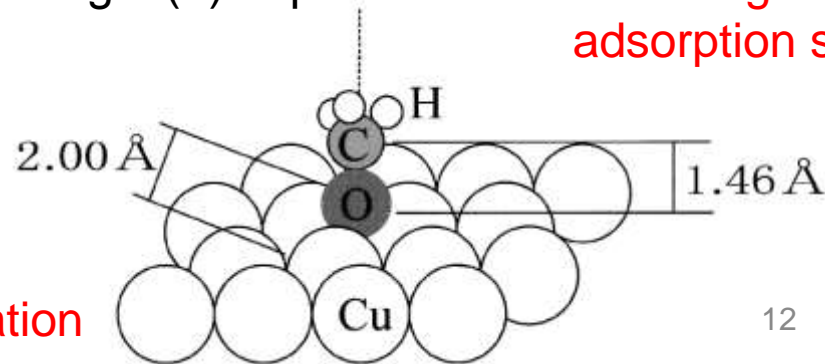
Angle (θ) dependence -> **molecular orientation**

Application to surface molecule (CH_3O)



Oscillation period -> **O-Cu bond length**

Angle (θ) dependence -> **bond angle**
adsorption site



Magnetic structures studied by XMCD

3 ML Fe / Cu(100)
Fe L-edge XMCD

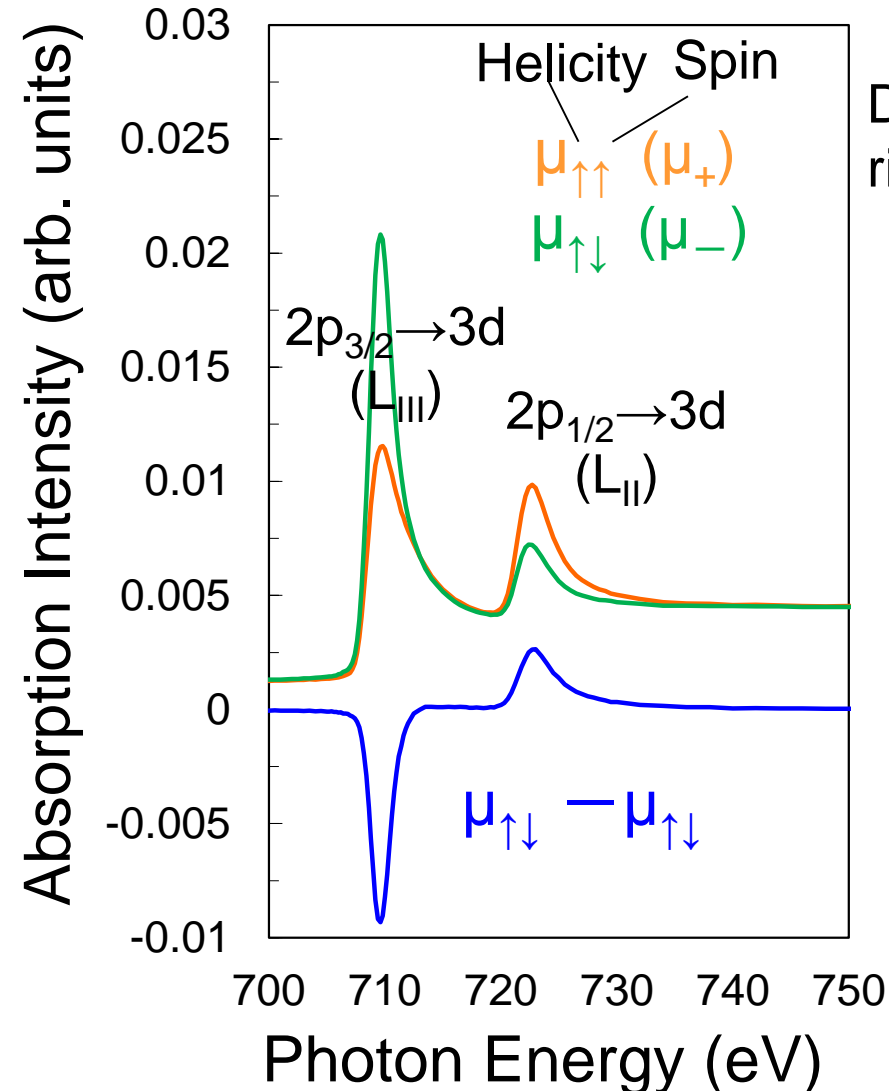
X-ray Magnetic Circular Dichroism (XMCD)

Difference in absorption intensities between right- and left-hand circular polarizations

1. **Element selectivity**
← resonant absorption ($2p \rightarrow 3d \dots$)
2. Determination of **spin and orbital magnetic moments**
← **Sum rules**
3. High sensitivity

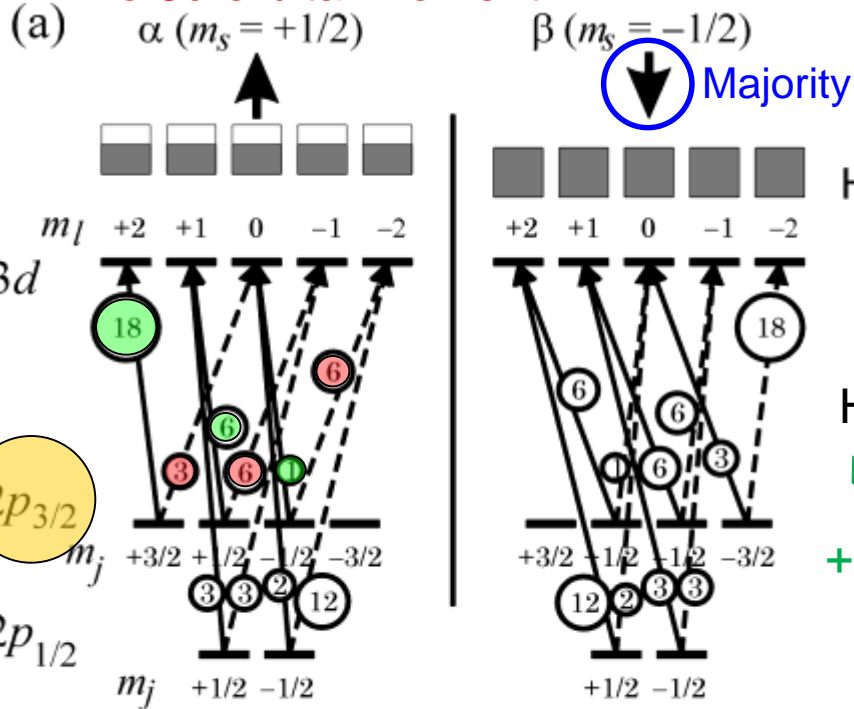
Element-specific **vector average** of magnetic moment over the whole investigation area

Fe \uparrow Gd \downarrow Fe \uparrow Gd \downarrow → Fe and Gd XMCD
Fe \uparrow Gd \uparrow Fe \uparrow Gd \downarrow → no Gd XMCD



Principle of XMCD

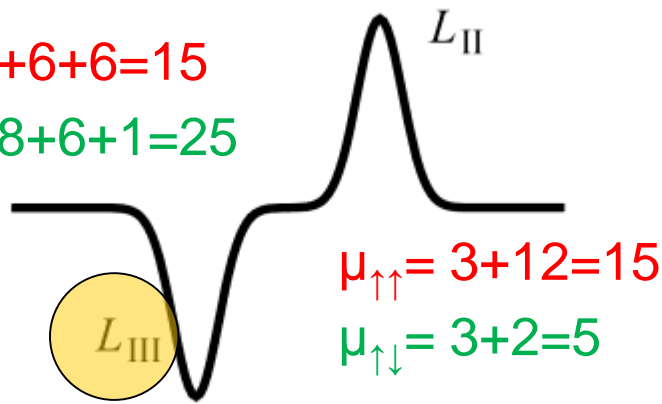
No 3d orbital moment



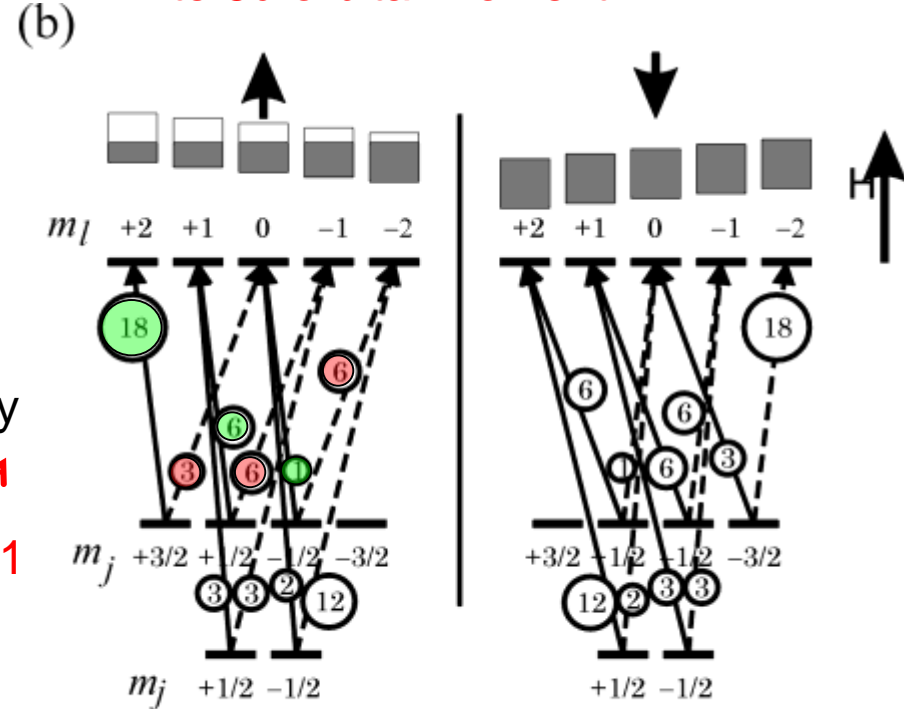
Dipole transition probability

$$\mu_{\uparrow\uparrow} = 3+6+6=15$$

$$\mu_{\uparrow\downarrow} = 18+6+1=25$$

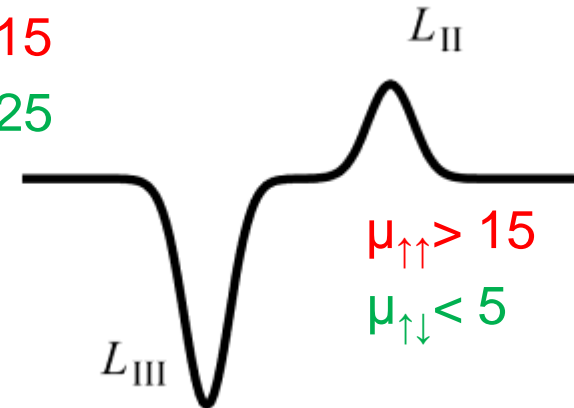


Finite 3d orbital moment

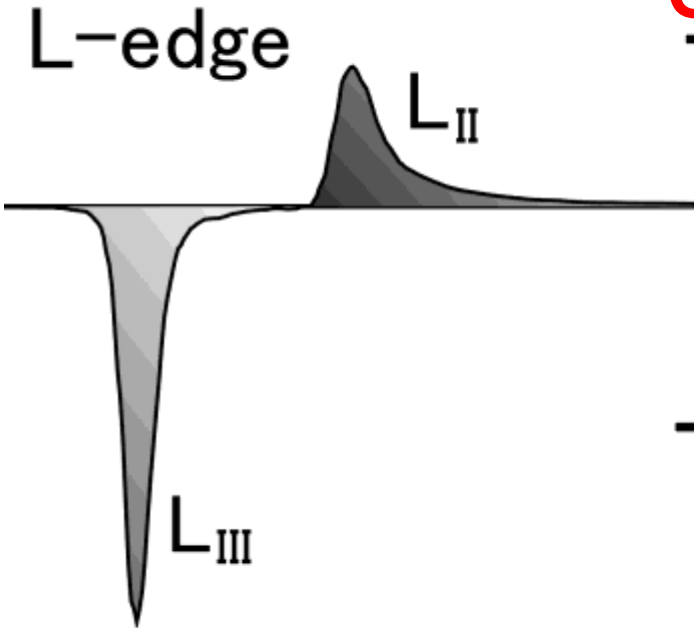


$$\mu_{\uparrow\uparrow} < 15$$

$$\mu_{\uparrow\downarrow} > 25$$



XMCD Sum Rules



Orbital moment m_l

$$\int L_{III}(\mu_+ - \mu_-) + \int L_{II}(\mu_+ - \mu_-)$$

$$\langle 0 \rightarrow m_l \rangle > 0$$

Spin moment m_s

$$\int L_{III}(\mu_+ - \mu_-) - 2 \int L_{II}(\mu_+ - \mu_-)$$

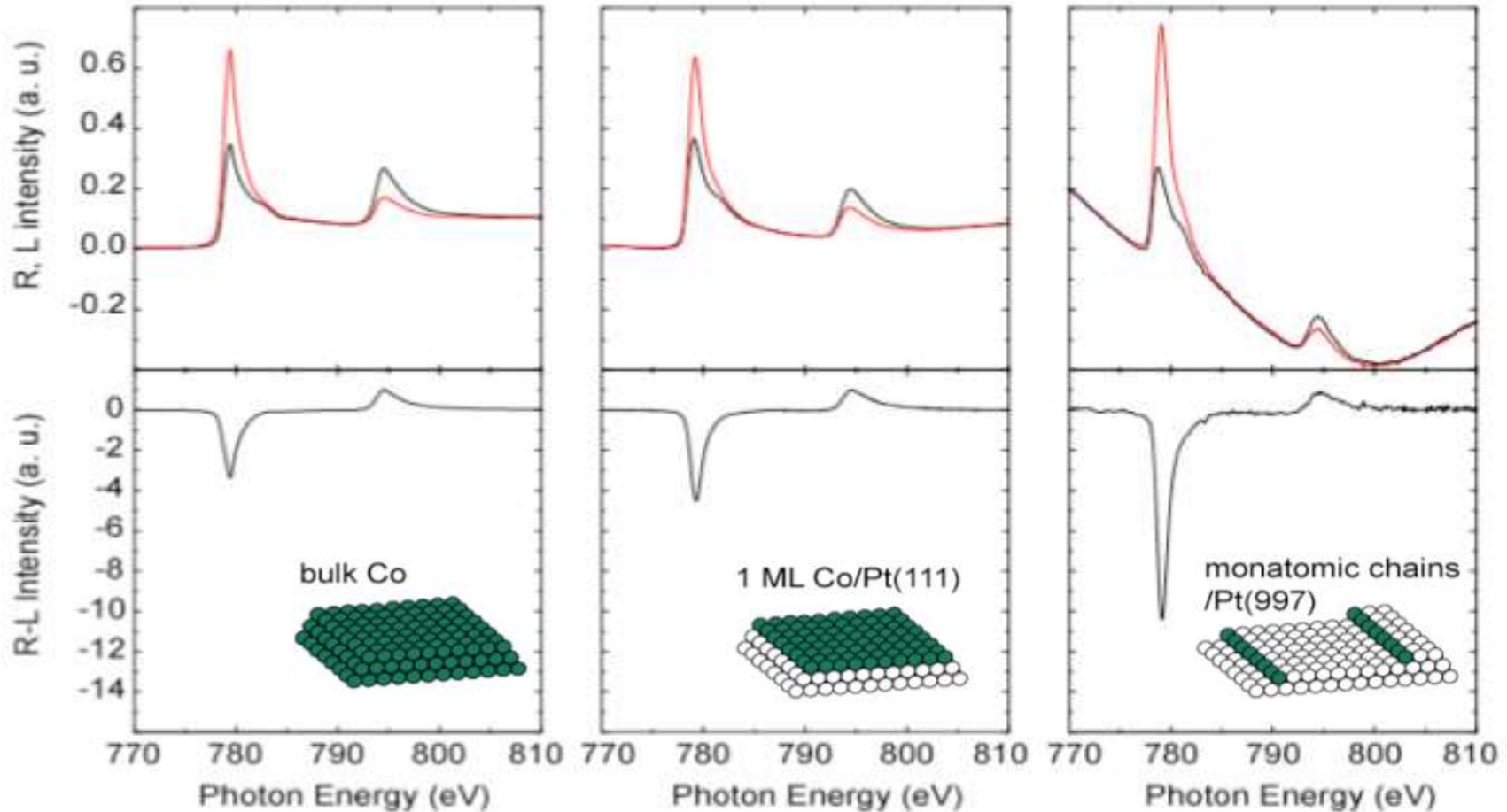
$$\langle 0 \rightarrow m_s \rangle > 0$$

B.T. Thole et al., PRL **68**, 1943 (1992).
P. Carra et al., PRL **70**, 694 (1993).

Magnetism of Thin Films Studied by XMCD

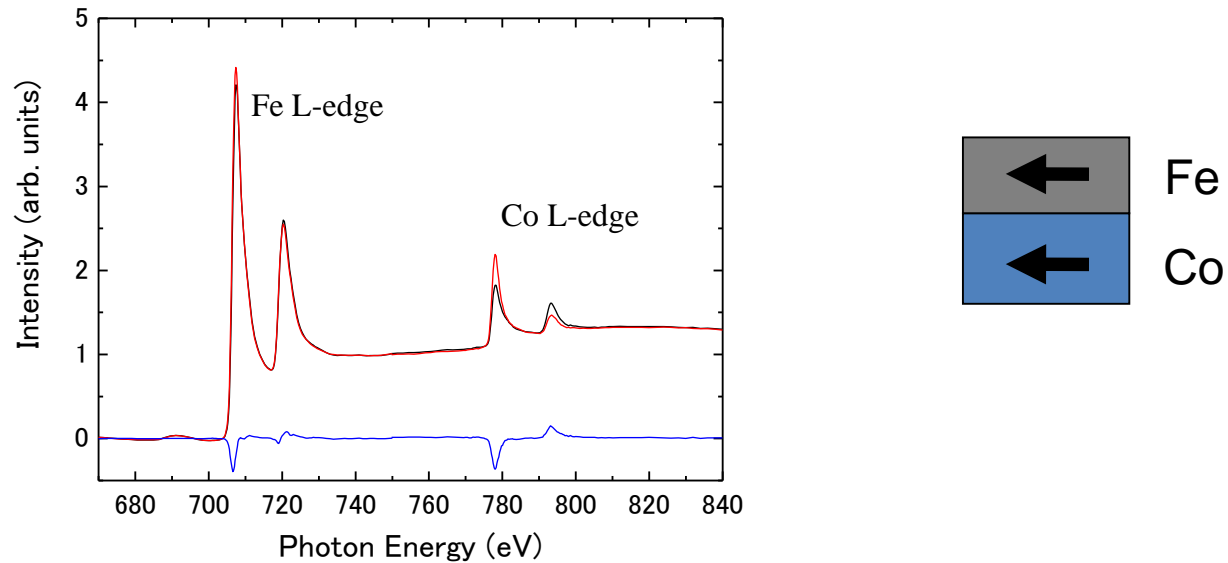
Co L-edge XMCD spectra

P. Gambardella, Nature **416**, 301 (2002)

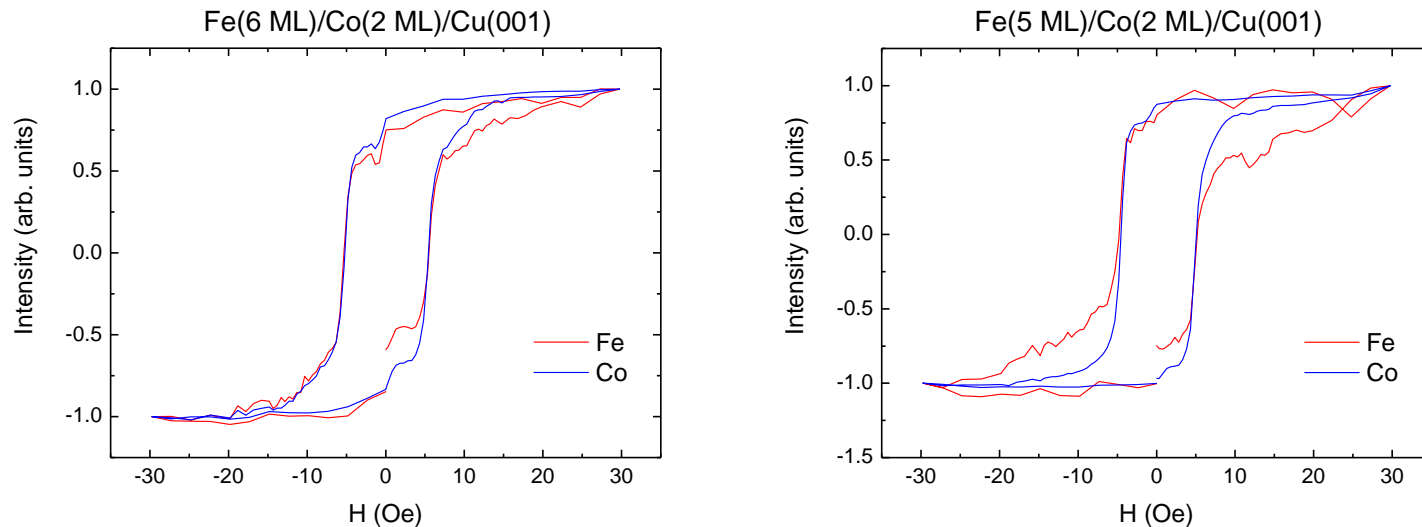


Larger orbital moment, m_l ,
due to lower dimension

Utilization of Element Selectivity of XMCD

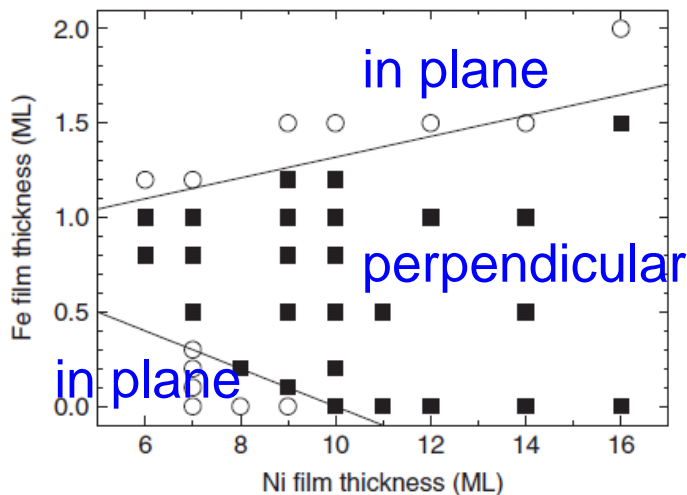
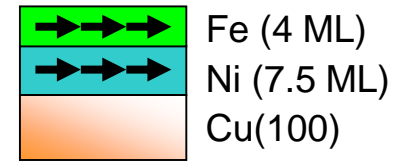
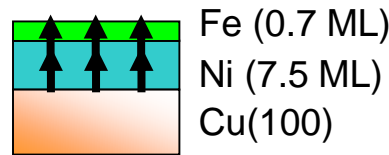
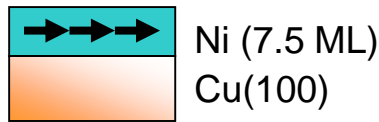
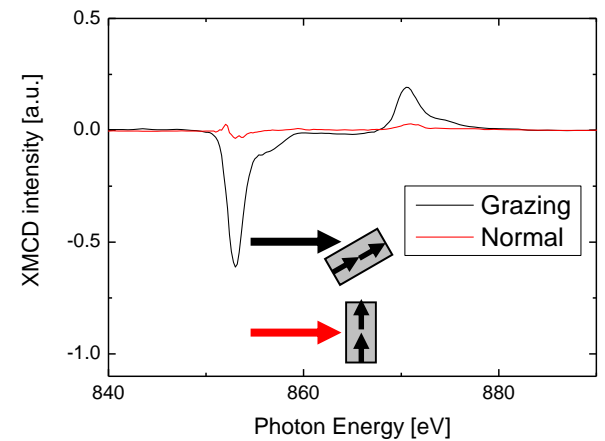
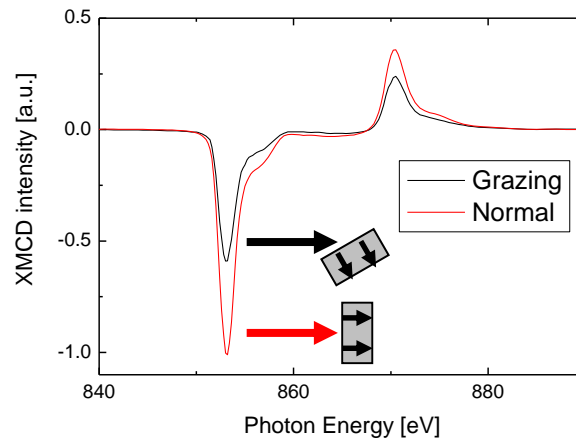
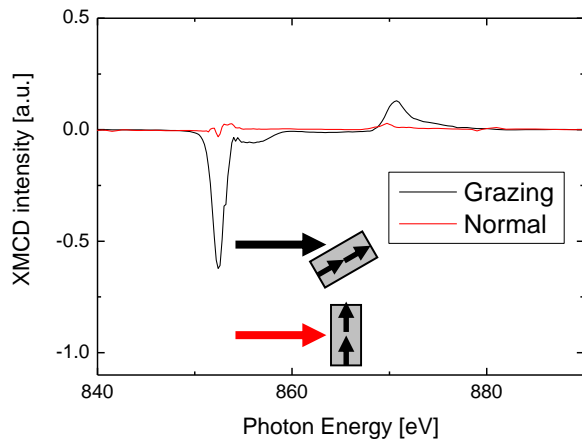


Magnetic-field dependence of XMCD at Fe and Co L edges



Angle Dependence of XMCD

(1) Weak magnetic field or remanent measurements



XMCD reflects magnetic component which is **parallel to X-ray beam**.

→ determination of easy axis of magnetization

Information on anisotropy of orbital moment

→ estimation of **magnetic anisotropy**

Abe et al., J. Magn. Magn. Mater. 206 (2006) 86.

Sakamaki and Amemiya, Appl. Phys. Express 4 (2011) 073002.

Sakamaki and Amemiya, Phys. Rev. B 87 (2013) 014428.

Angle Dependence of XMCD

(2) High magnetic field measurements

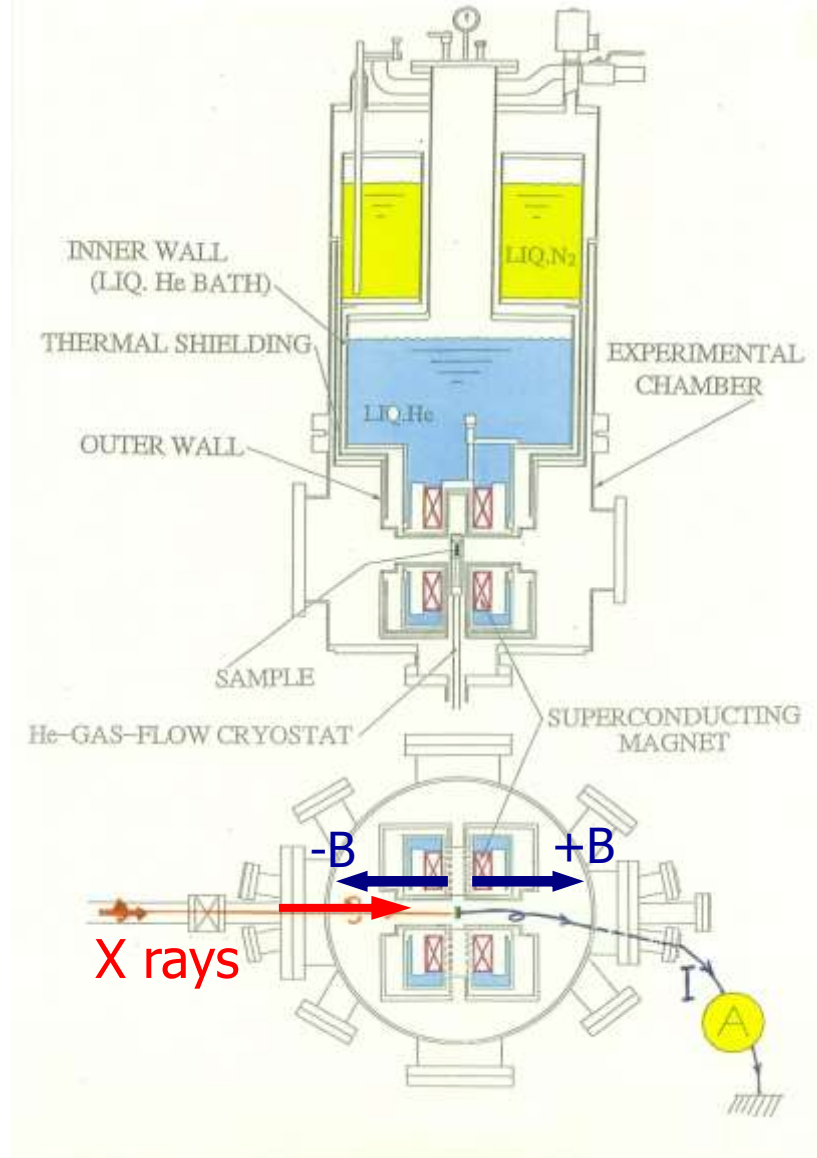
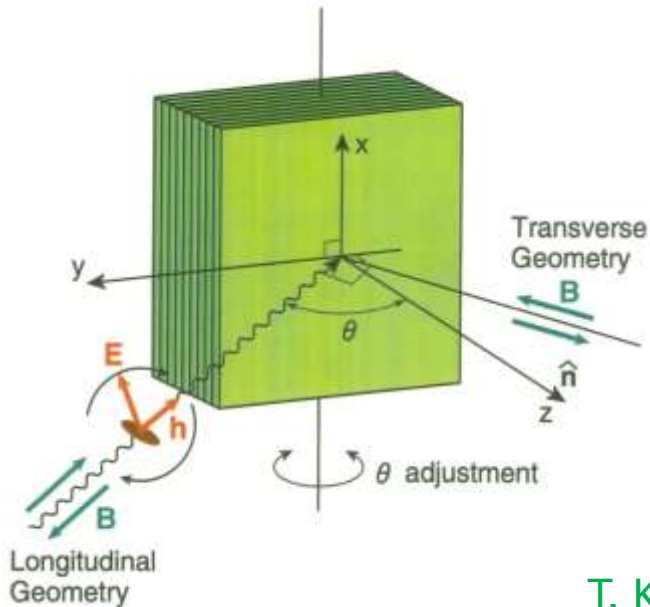
Angle-dependent XMCD

=> **Magnetic anisotropy**

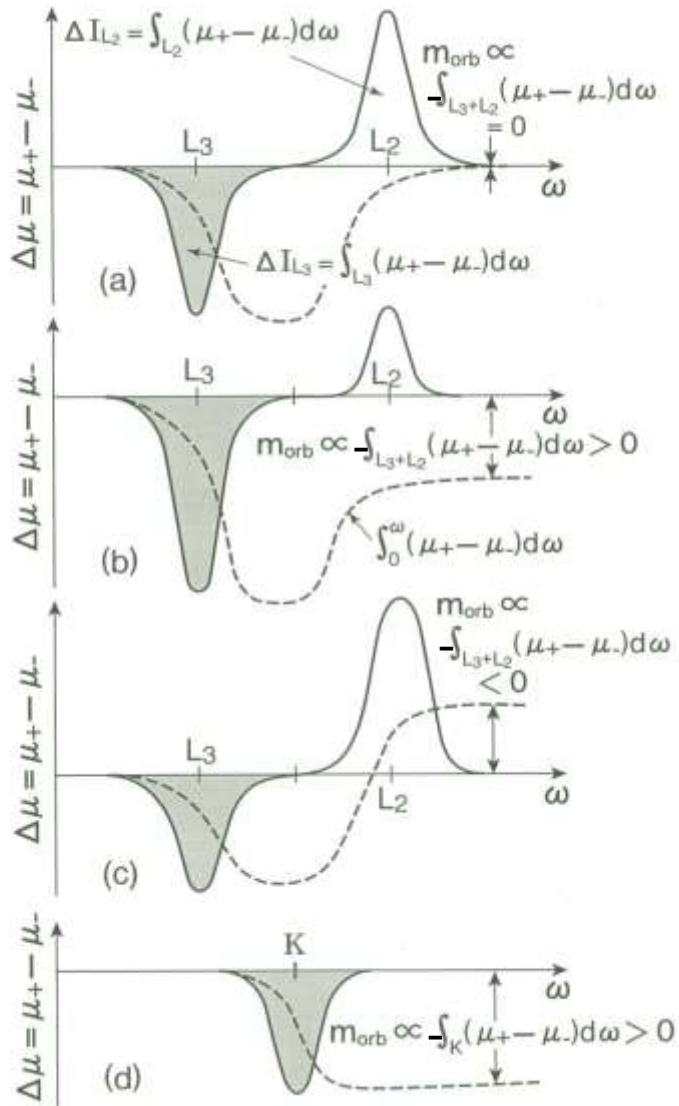
Direct determination of m_s and m_T

m_T : dipole magnetic moment

$$\mathbf{T} = \sum_i \mathbf{s}_i - 3\mathbf{r}_i(\mathbf{r}_i \cdot \mathbf{s}_i) / r_i^2.$$



Angle-dependent XMCD Sum Rules



Orbital sum rule

$$\frac{[\Delta I_{L_3} + \Delta I_{L_2}]^\theta}{I_{L_3} + I_{L_2}} = - \frac{3 \cdot m_l^\theta}{4n_h \cdot \mu_B}$$

Spin sum rule

$$\frac{[\Delta I_{L_3} - 2 \cdot \Delta I_{L_2}]^\theta}{I_{L_3} + I_{L_2}} = - \frac{(m_s + 7 \cdot m_T^\theta)}{2n_h \cdot \mu_B}$$

B.T. Thole et al., PRL **68**, 1943 (1992).
 P. Carra et al., PRL **70**, 694 (1993).

$$m_l^\theta = m_l^\perp \cos^2 \theta + m_l^\parallel \sin^2 \theta$$

$$m_T^\theta = m_T^\perp \cos^2 \theta + m_T^\parallel \sin^2 \theta$$

m_s does not depend on θ

⇒ Direct determination of

$$m_s, m_l^\parallel, m_l^\perp, m_T^\parallel, m_T^\perp$$

Investigation of Interface Magnetism

T. Koide et al., Phys. Rev. Lett. 87, 257201 (2001).

Au/Co(2 ML)/Au(111)

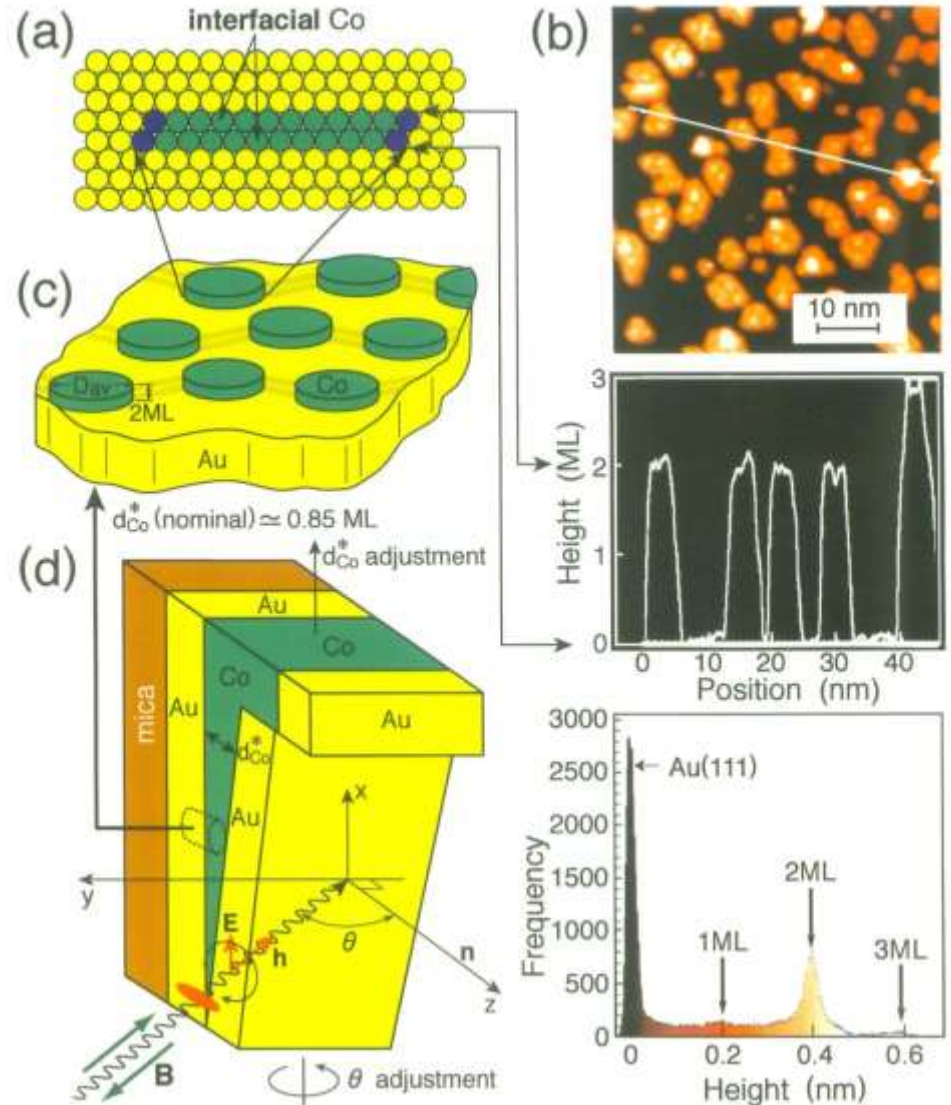
Self-assembled Co islands
due to a reconstruction of
Au surface

All Co atoms are regarded to
“interface” because of 2 ML
thickness

⇒ **Direct observation of
interface magnetism**

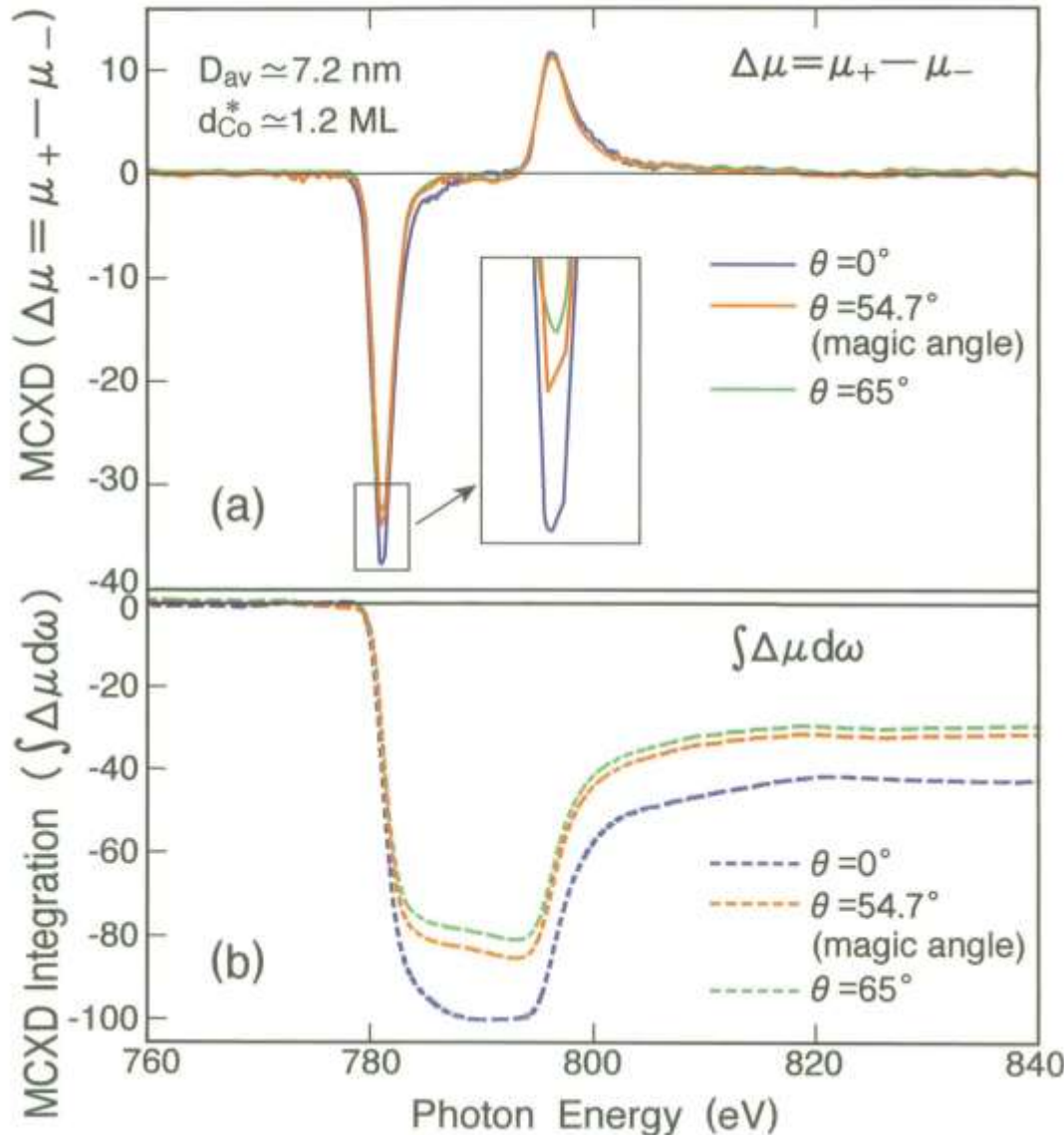
Determination of

m_s , m_i^{\parallel} , m_i^{\perp} , m_T^{\parallel} , m_T^{\perp}



Angle-dependent XMCD Measurements

T. Koide et al., Phys. Rev. Lett. 87, 257201 (2001).



PF BL-11A

Angle dependence in XMCD

← Anisotropy in m_l , m_T

$$m_j^\theta = m_j^\perp \cos^2\theta + m_j^\parallel \sin^2\theta$$

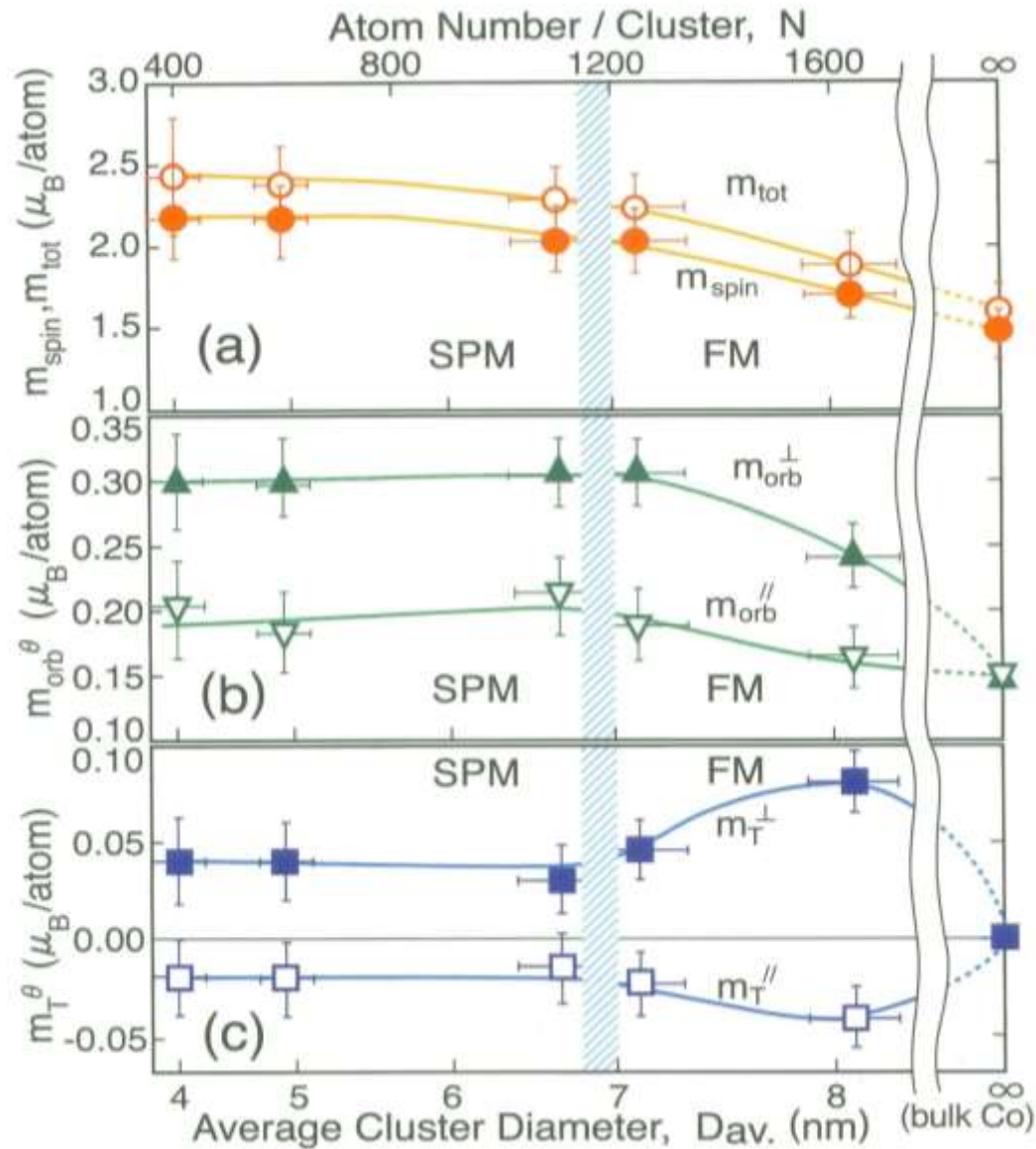
$(j = l \text{ or } T)$

$$m_T^\perp + 2 m_T^\parallel = 0$$

⇒ Determination of all moments including their **anisotropy**

Determined Magnetic Moments

T. Koide et al., Phys. Rev. Lett. 87, 257201 (2001).



Cluster-size dependent phase transition

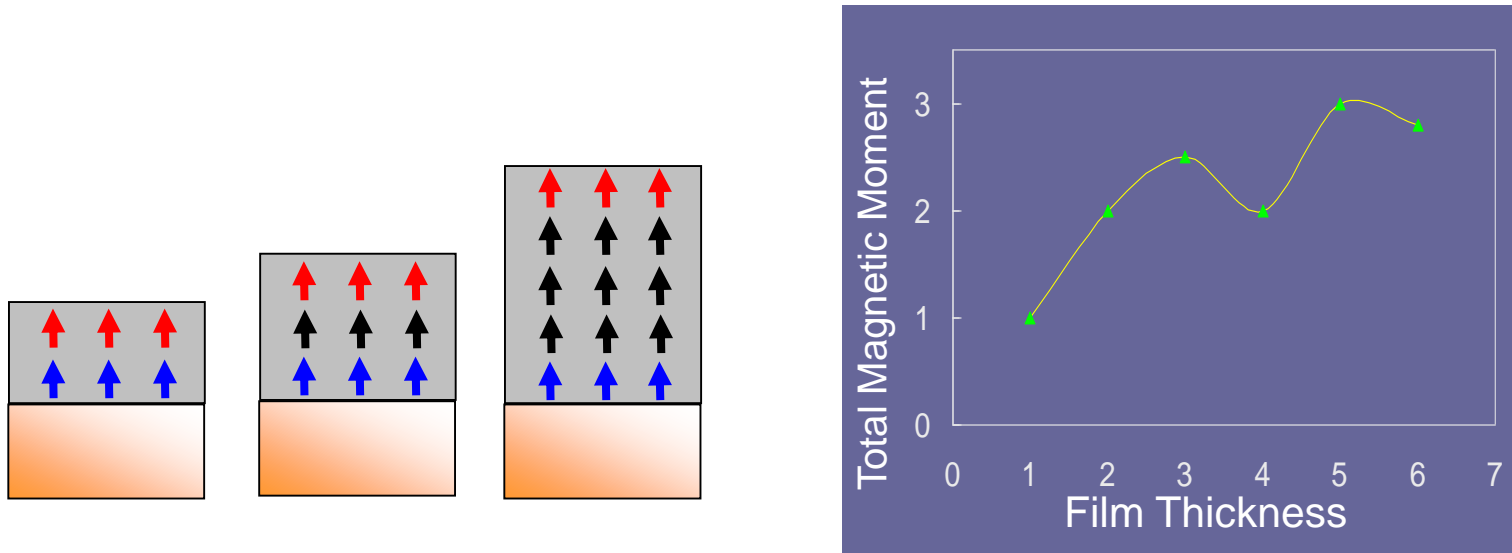
FM: ferromagnetic
SPM: super-paramagnetic

1. Advantages and Disadvantages of
Soft X-ray Absorption Spectroscopy (SXAS)
2. SXAS studies on Surface and Thin films
3. Novel SXAS Techniques
 - 3-1. Depth-resolved XAS
 - 3-2. Wavelength-dispersive XAS

Conventional Technique for Depth Profiling

SQUID, VSM, MOKE, XMCD...

Gives **averaged information** over the whole sample.
⇒ also **averaged in depth**



Based on an **assumption**
that magnetic structure of surface and interface
dose not change upon layer growth

➔ **Direct technique for depth profiling**

Co/Cu(100) - Surface & interface orbital moment -

Tischer et al., Phys. Rev. Lett.
75 (1995) 1602.

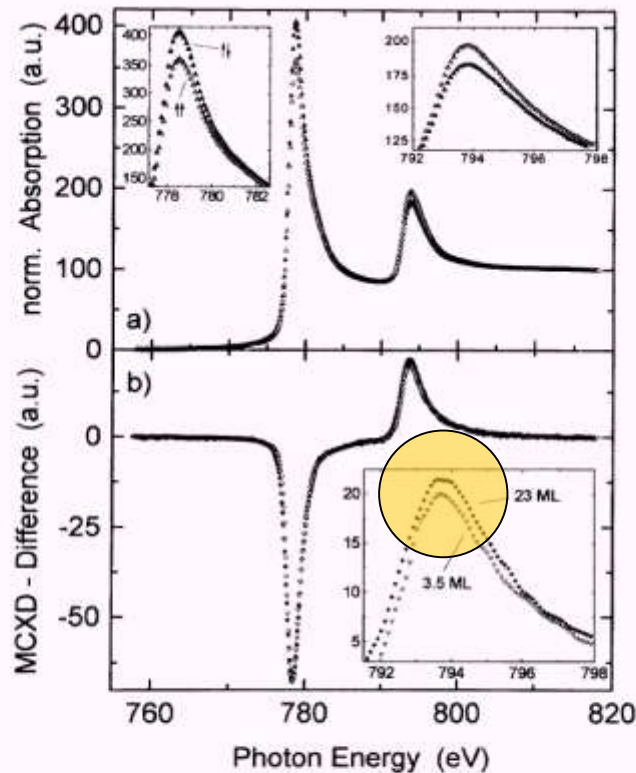


FIG. 2. (a) The normalized absorption spectrum for 3.5 ML Co/Cu(100). Open triangles indicate the photon spin parallel to the remanent magnetization, full triangles antiparallel. (b) MCXD difference for the 3.5 ML film (triangles) and a thick 23 ML film (circles). Both are normalized to the same L_3 intensity to demonstrate that the dichroic response around the L_2 edge is relatively smaller for the thin film.

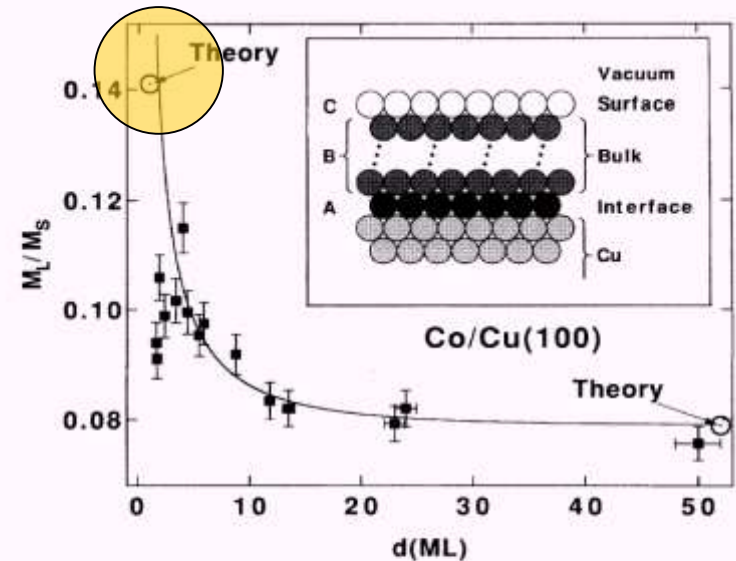
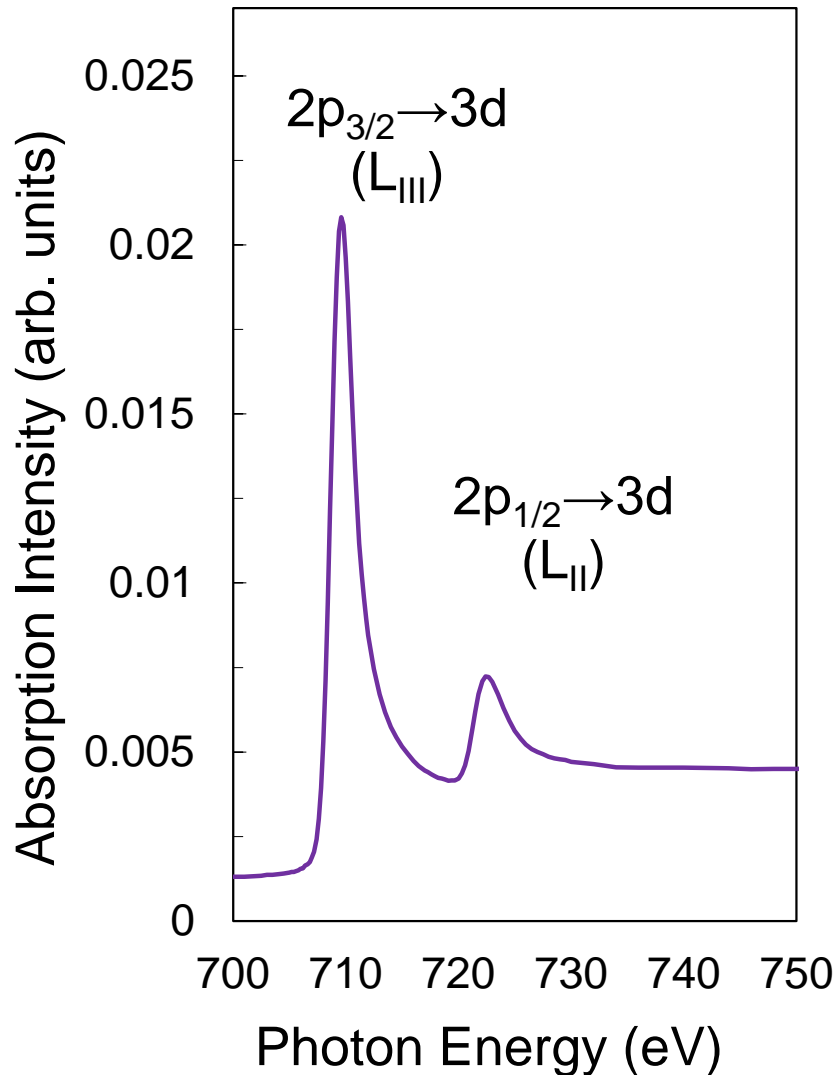


FIG. 3. The ratio of orbital versus spin moment M_L/M_S as a function of film thickness d . The open circles give the theory taken from Table I. The full squares show the experiment. The solid line is a fit using Eq. (1) with the parameters given in the last row of Table I. Note that the fit was performed only for $d \geq 3$ ML, corresponding to well-defined, epitaxial growth. The surface, interface, and bulk contributions used in Eq. (1) are schematically shown in the inset.

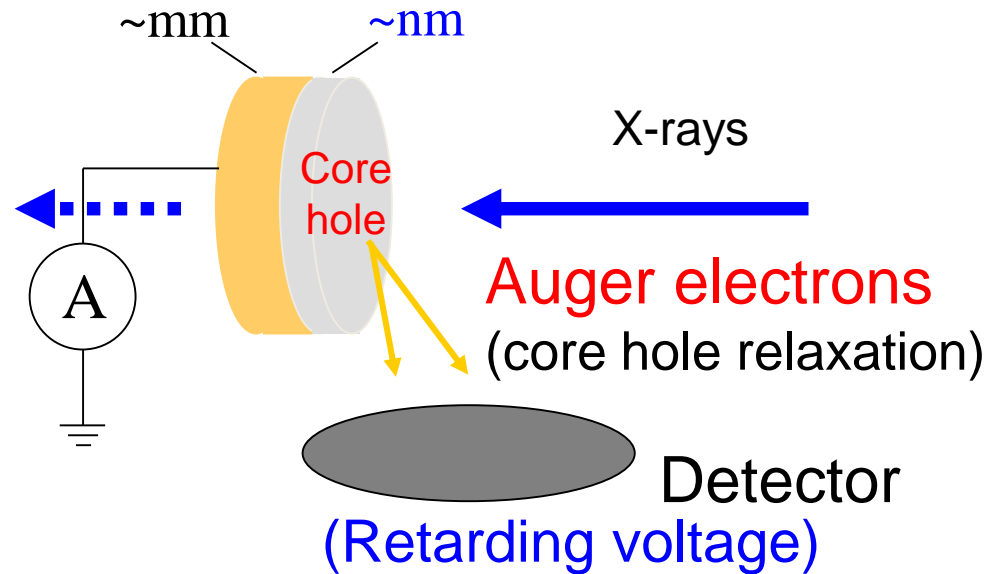
XAS Measurement in the Soft X-ray Region

3 ML Fe / Cu(100) **Fe L-edge XAS**



How can we measure

X-ray absorption spectrum ?



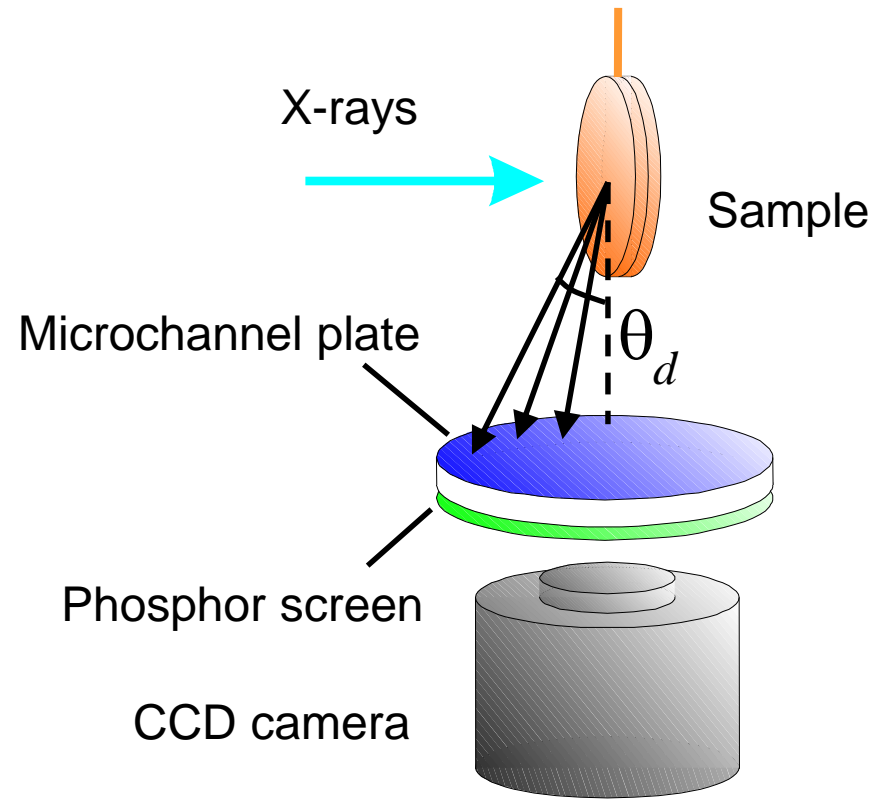
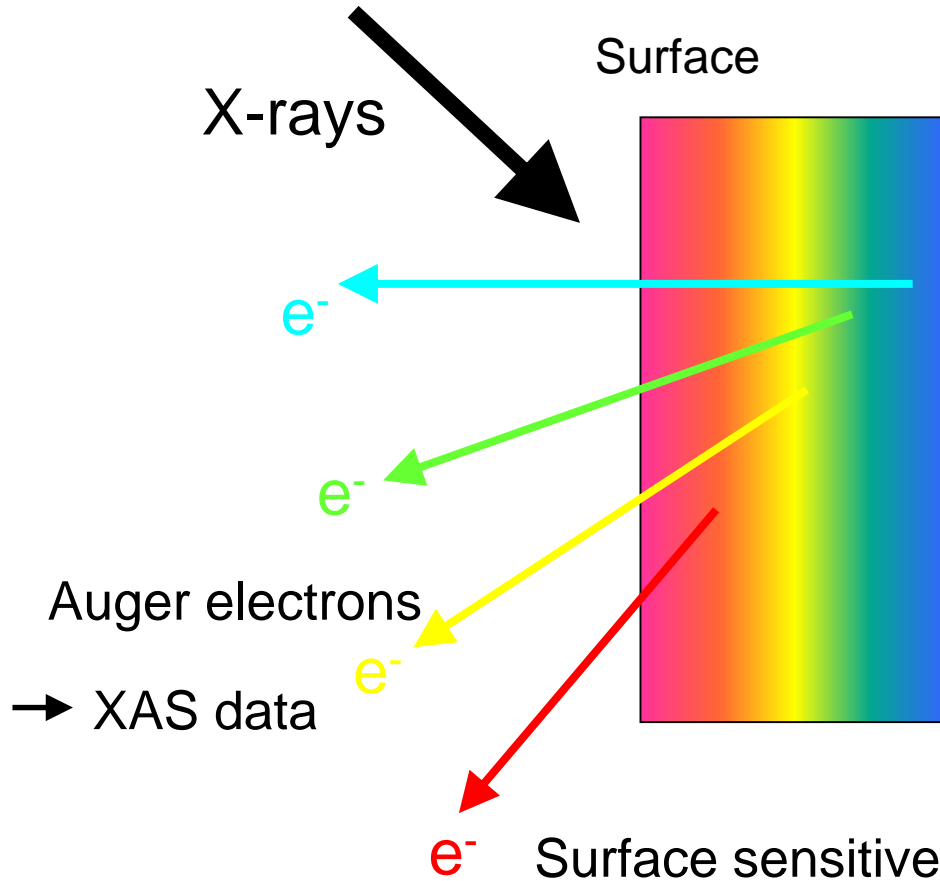
Electron yield XAS

Total electron yield (TEY)

Partial electron yield (PEY)

cf. **Fluorescence yield (FY)**

Principle of Depth-resolved XAS



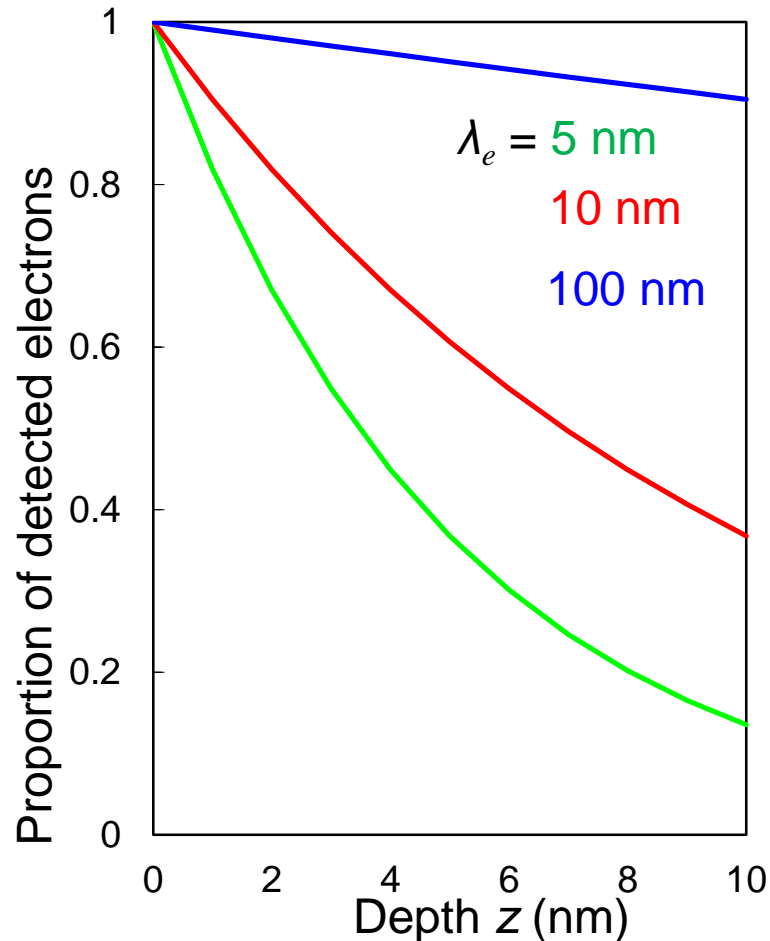
Electron yield XAS measurements at different detection angles, θ_d

→ A set of XAS data with different probing depths

Probing Depth (effective escape depth): λ_e

Number of detected electrons emitted at depth z : $I = I_0 \exp(-z/\lambda_e)$

I_0 : Original number of emitted electrons



Smaller λ_e

\Rightarrow Larger contribution from **surface**

XAS:

Averaged information **per atom**

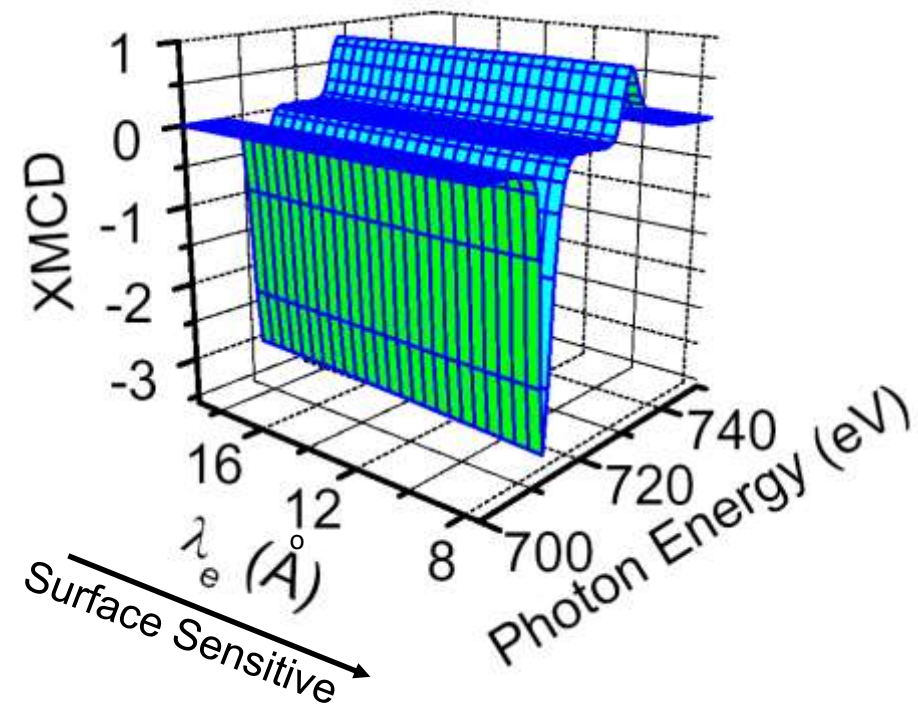
Depth-resolved XAS:

$\exp(-z/\lambda_e)$ -**weighted average**

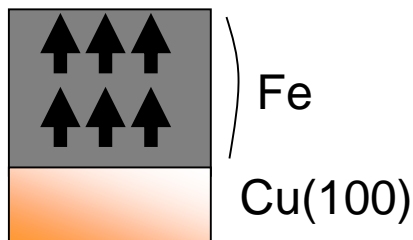
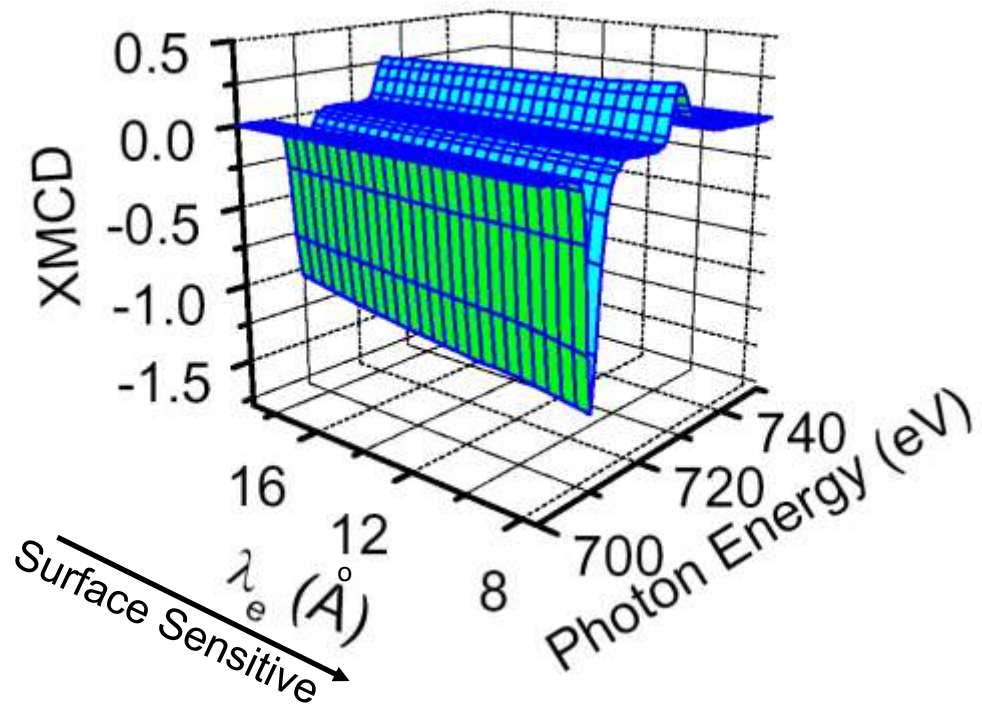
Feasibility Study: Depth-resolved XMCD of Fe/Cu(100)

Amemiya et al., Appl. Phys. Lett. 84 (2004) 936. Normal Incidence, 130 K

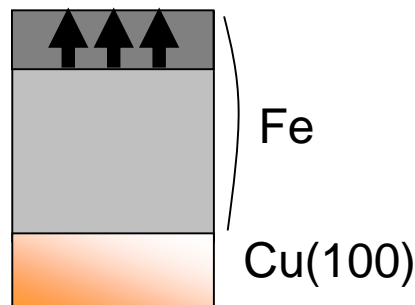
3 ML Fe



7 ML Fe

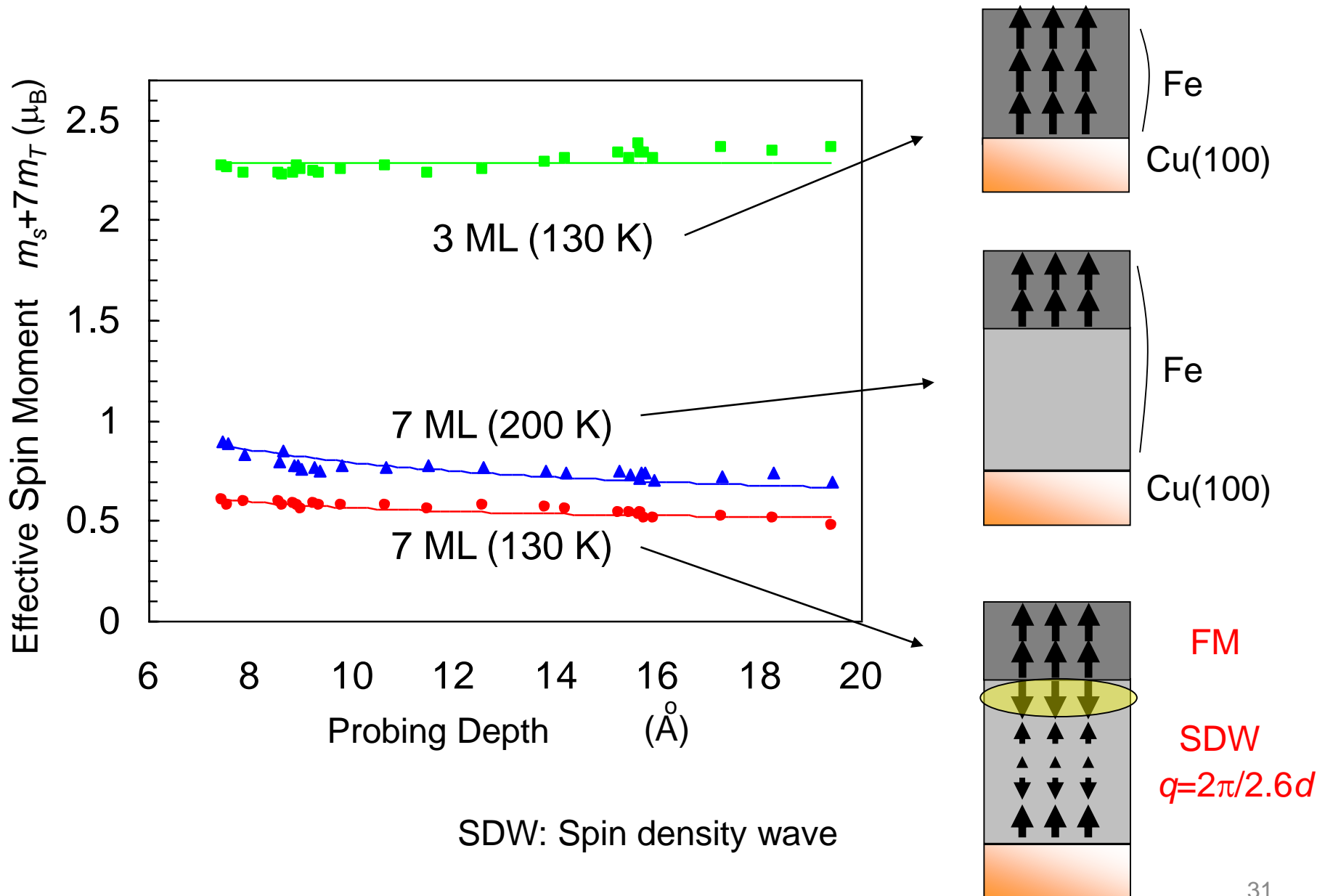


Uniform
Magnetization

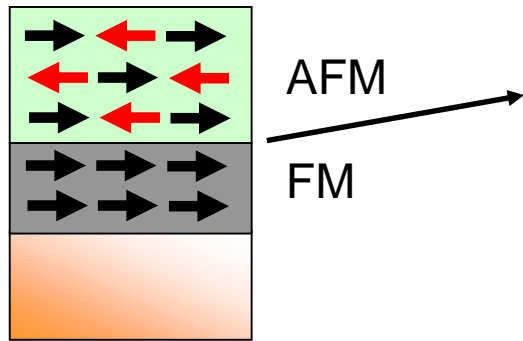


Surface
Magnetization

Interpretation of depth-resolved XMCD data



Application 1: Ferromagnetic/Antiferromagnetic interface

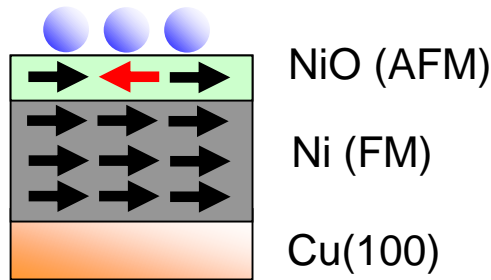
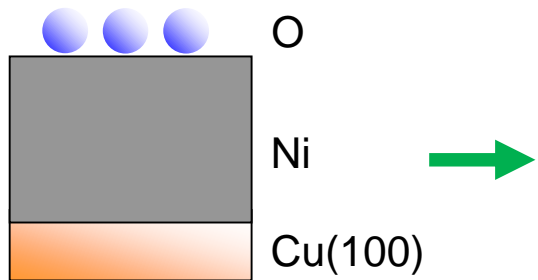


Exchange bias
 Uncompensated spin
 Intermixing
 Roughness

Atomically sharp interface
 is desirable

...

Idea of our study



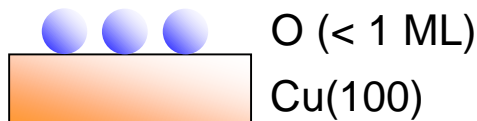
Single-layer NiO ?
 Ideal FM-AFM interface

Sample preparation

R. Nunthel et al., Surf. Sci. 531, 53 (2003).

(1) Oxygen adsorption

5×10^{-4} Pa, 300 s @ 500 K

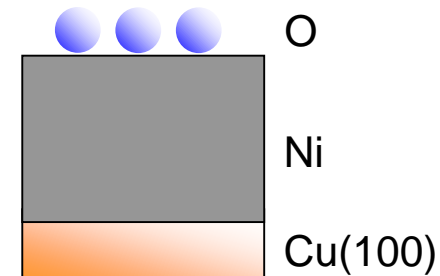


(2) Ni deposition (in UHV)

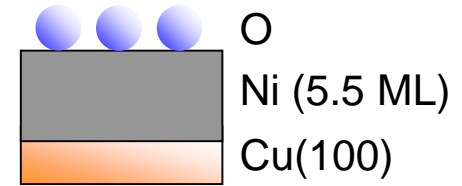
EB heating of a Ni rod

room temperature

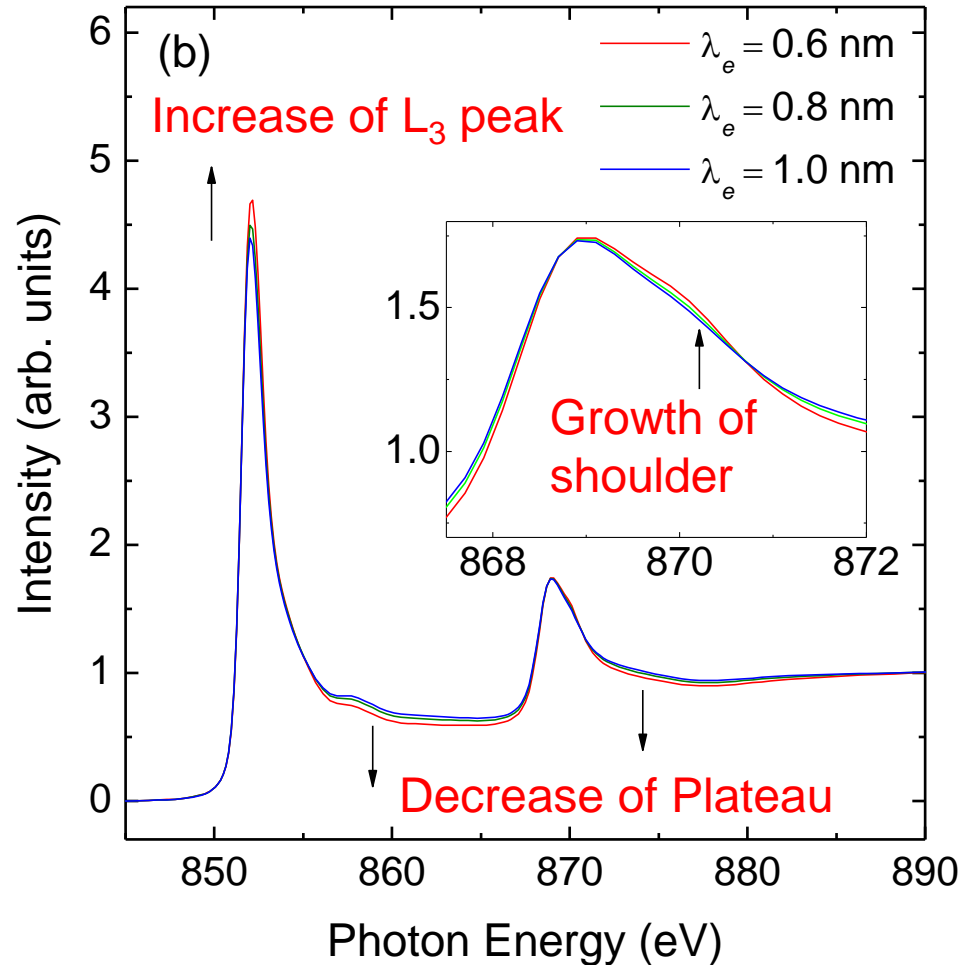
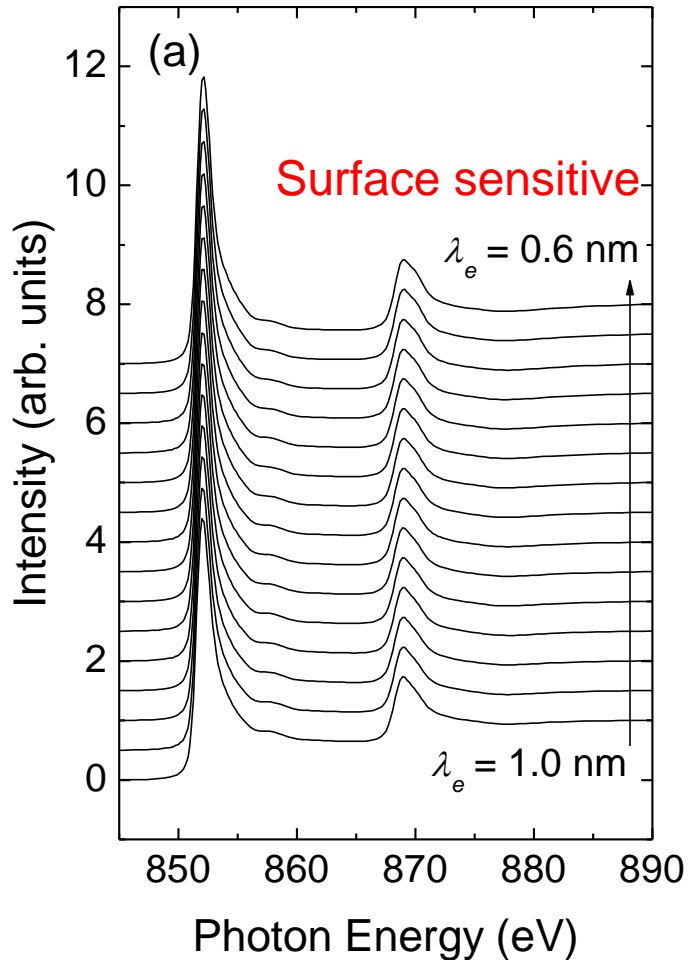
in situ RHEED



Depth-resolved XAFS for O/Ni/Cu(100)

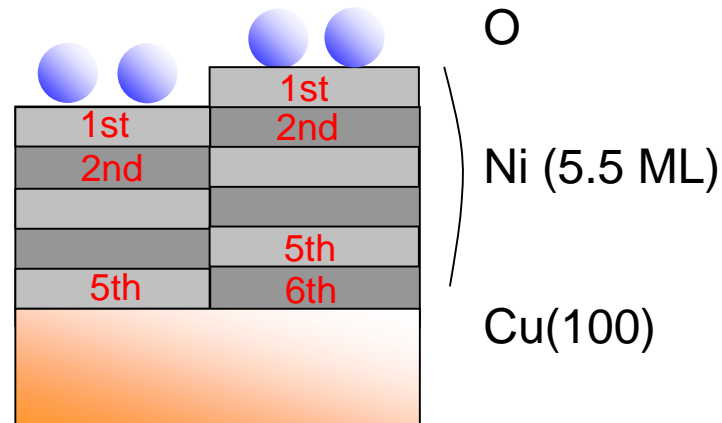
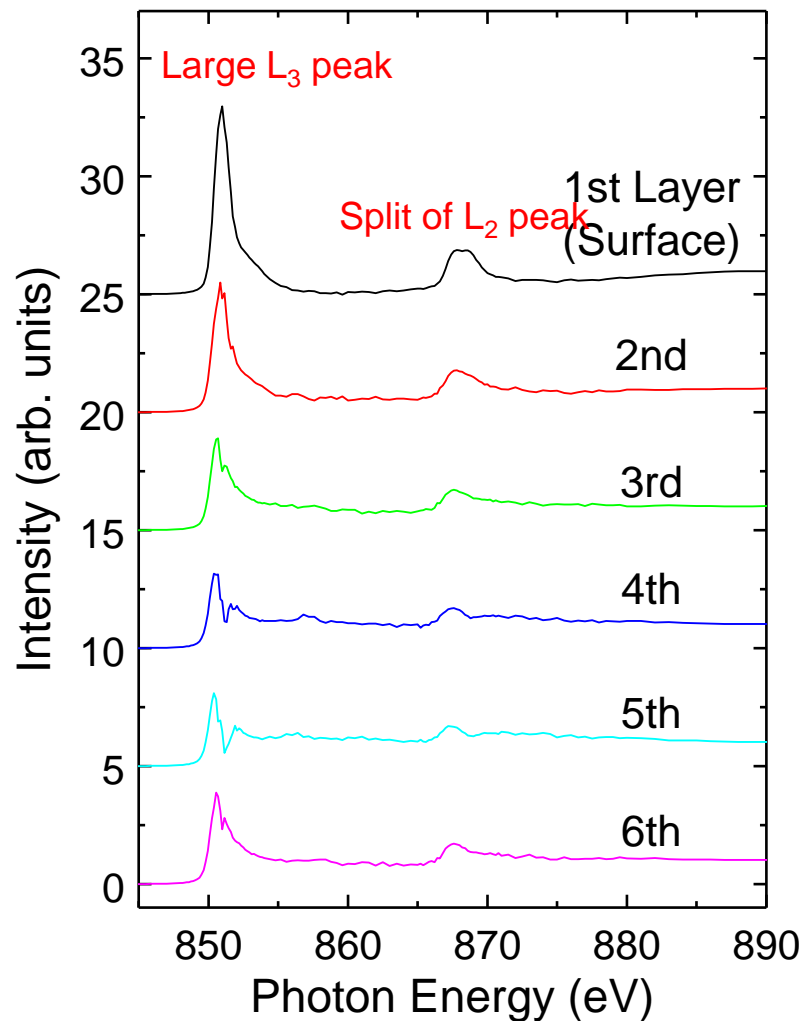


O/Ni(5.5 ML)/Cu(001) Ni L-edge XAS (X-ray Absorption Spectrum)



Layer-resolved X-ray absorption spectra

O/Ni(5.5 ML)/Cu(001)
Ni L-edge XAS ($E//x$) Extracted Spectra



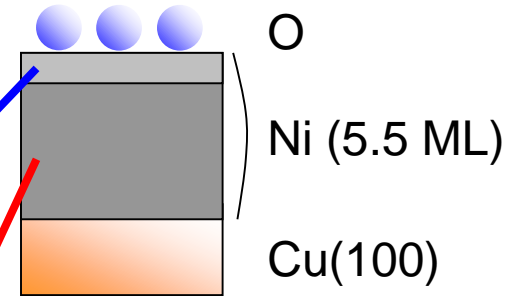
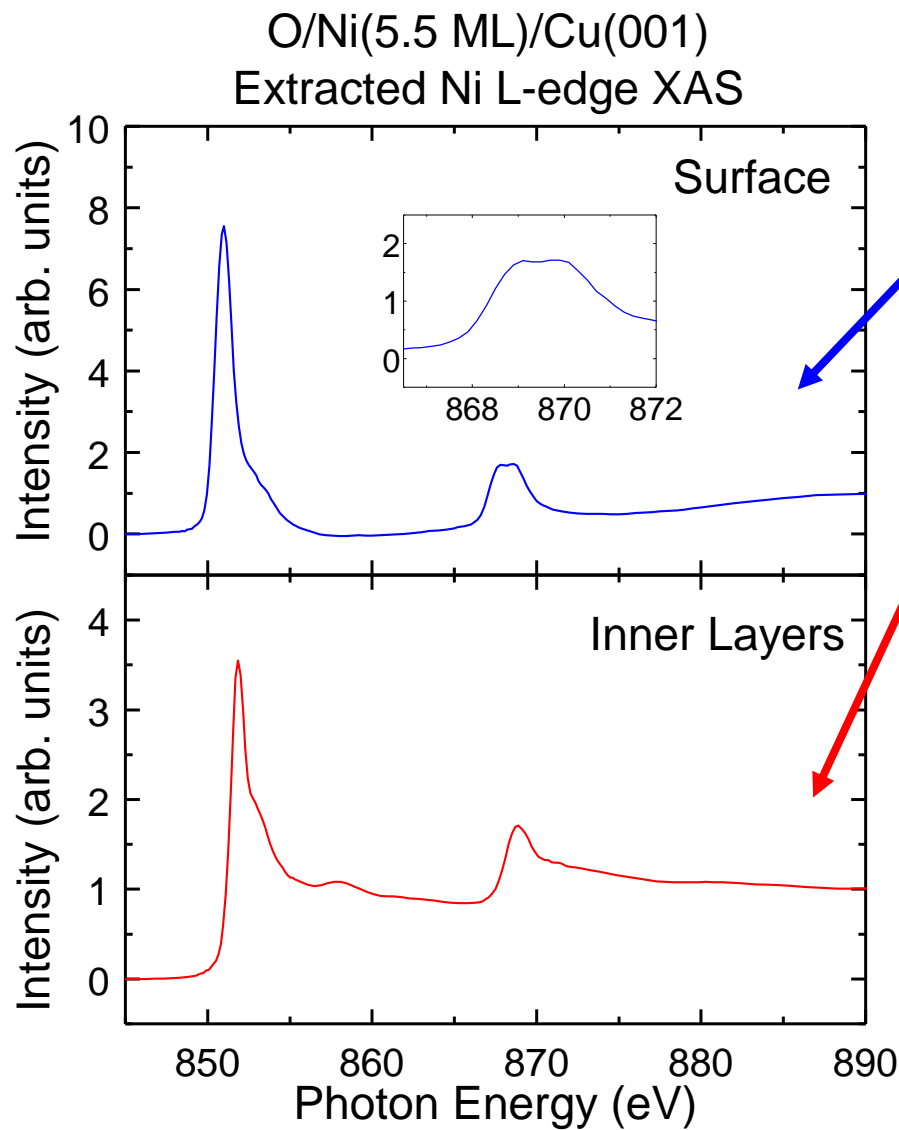
XAS for the 1st layer is different from those in the underlying layers

=> suggests **single-layer oxidation**

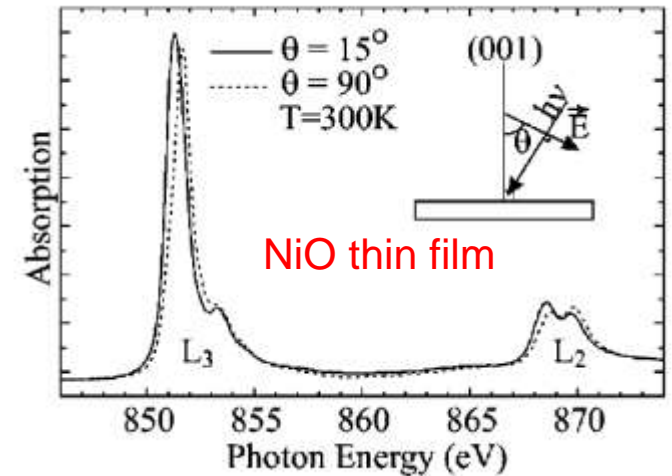
=> **2-region model** is adopted.

Extracted X-ray absorption Spectra

K. Amemiya and M. Sakamaki,
Appl. Phys. Lett. 98 (2011) 012501.

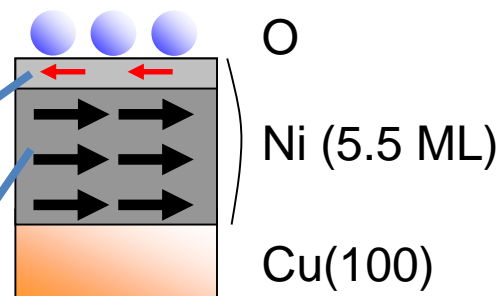
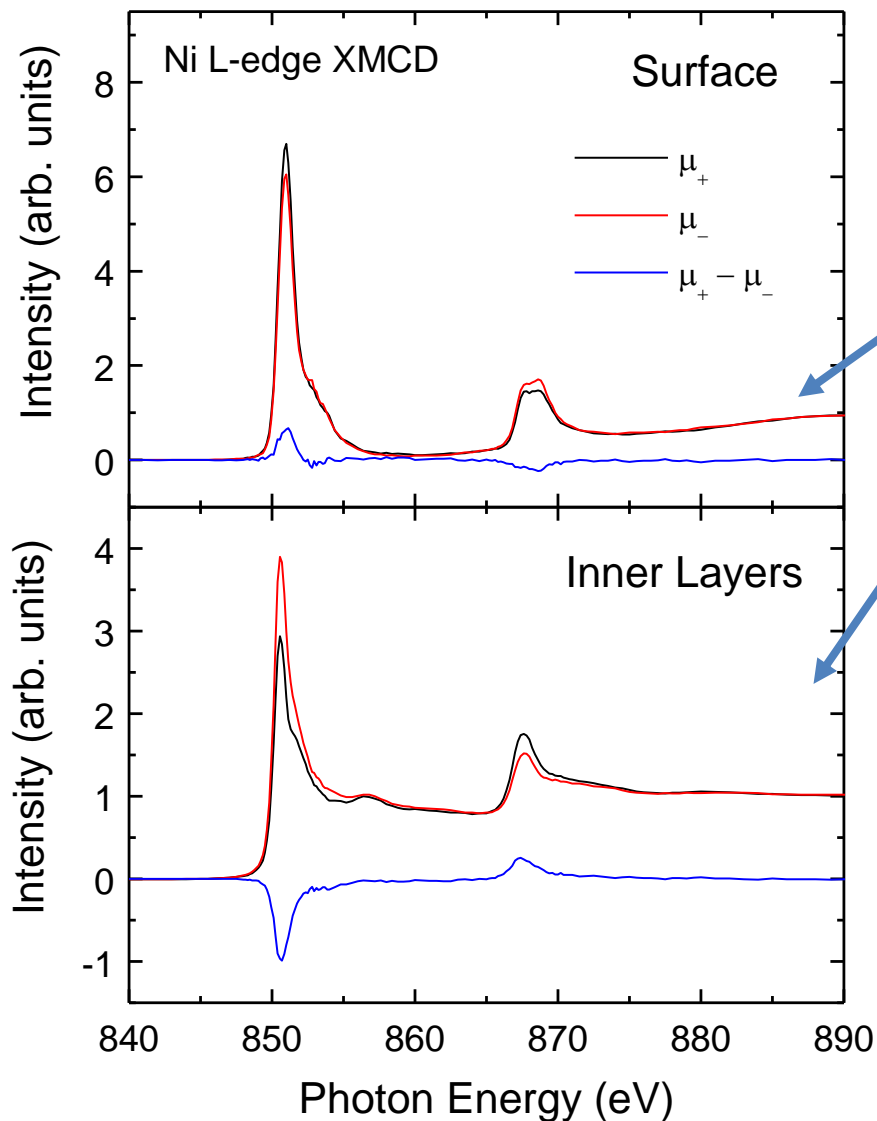


XAS spectra at surface
shows NiO-like features



Haverkort et al., Phys. Rev. B 69, 020408(R).

Extracted XMCD spectra



Surface layer shows small
negative magnetization.

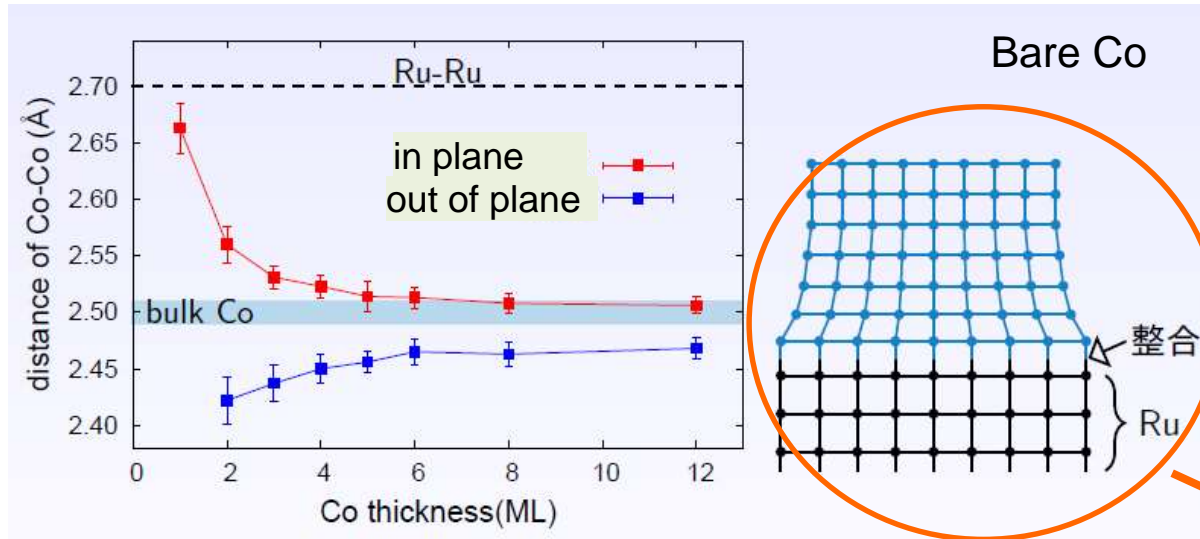
Uncompensated spin
at the interface?

K. Amemiya and M. Sakamaki,
Appl. Phys. Lett. 98 (2011) 012501.

Application 2: Atomic structure of Ru/Co/Ru(0001) thin films

Fluorescence-yield EXAFS (Co K edge) : average over the whole film

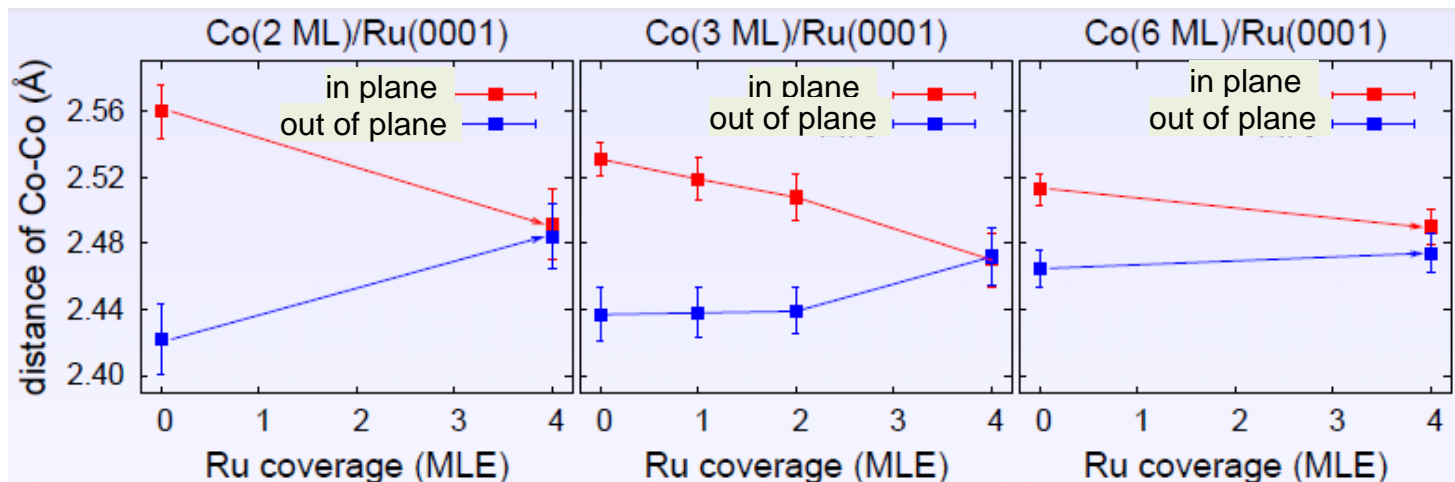
Miyawaki et al., Phys. Rev. B 80 (2009) 020408(R).



Interface Co layer is commensurate to Ru

Rapid relaxation upon further Co deposition

Effects of Ru capping



Is that true?

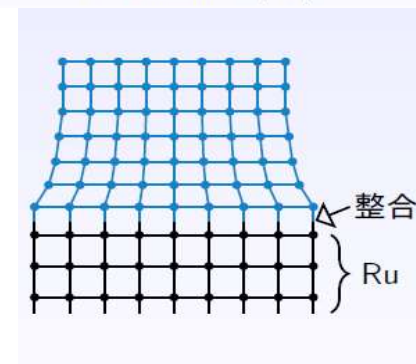
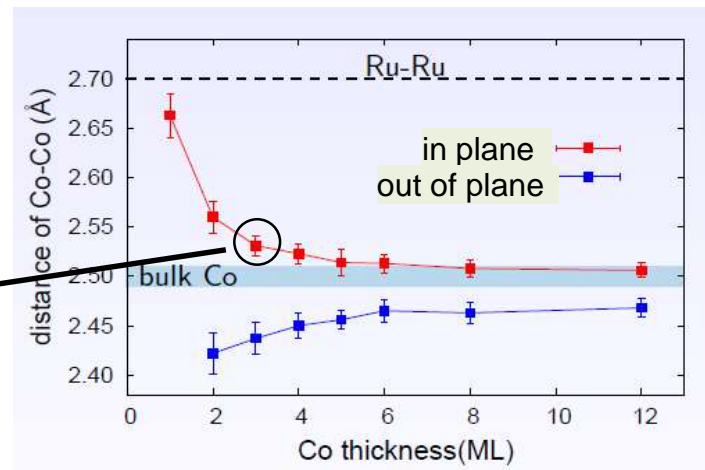
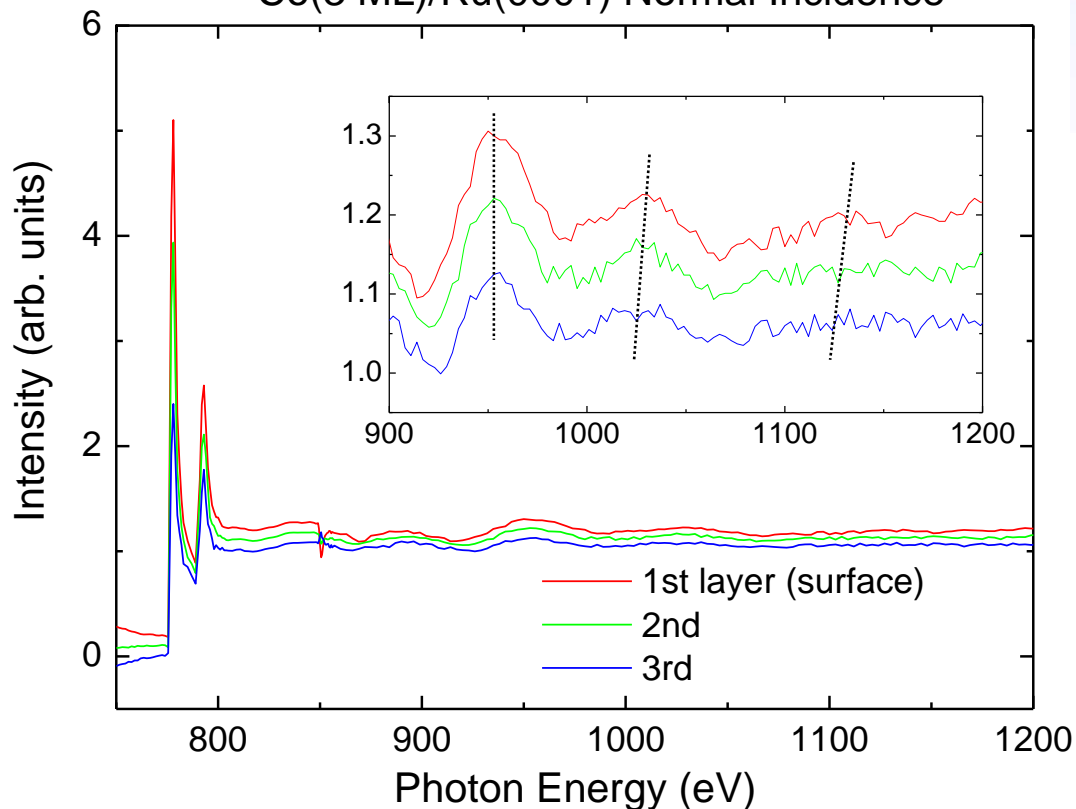
Relaxation of Co distortion upon Ru capping

Depth profile of atomic structure

Normal incidence: dominated by in-plane distance

Layer-resolved EXAFS

Co(3 ML)/Ru(0001) Normal Incidence



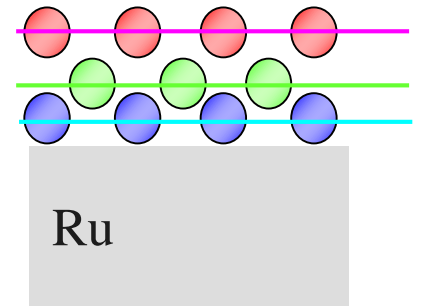
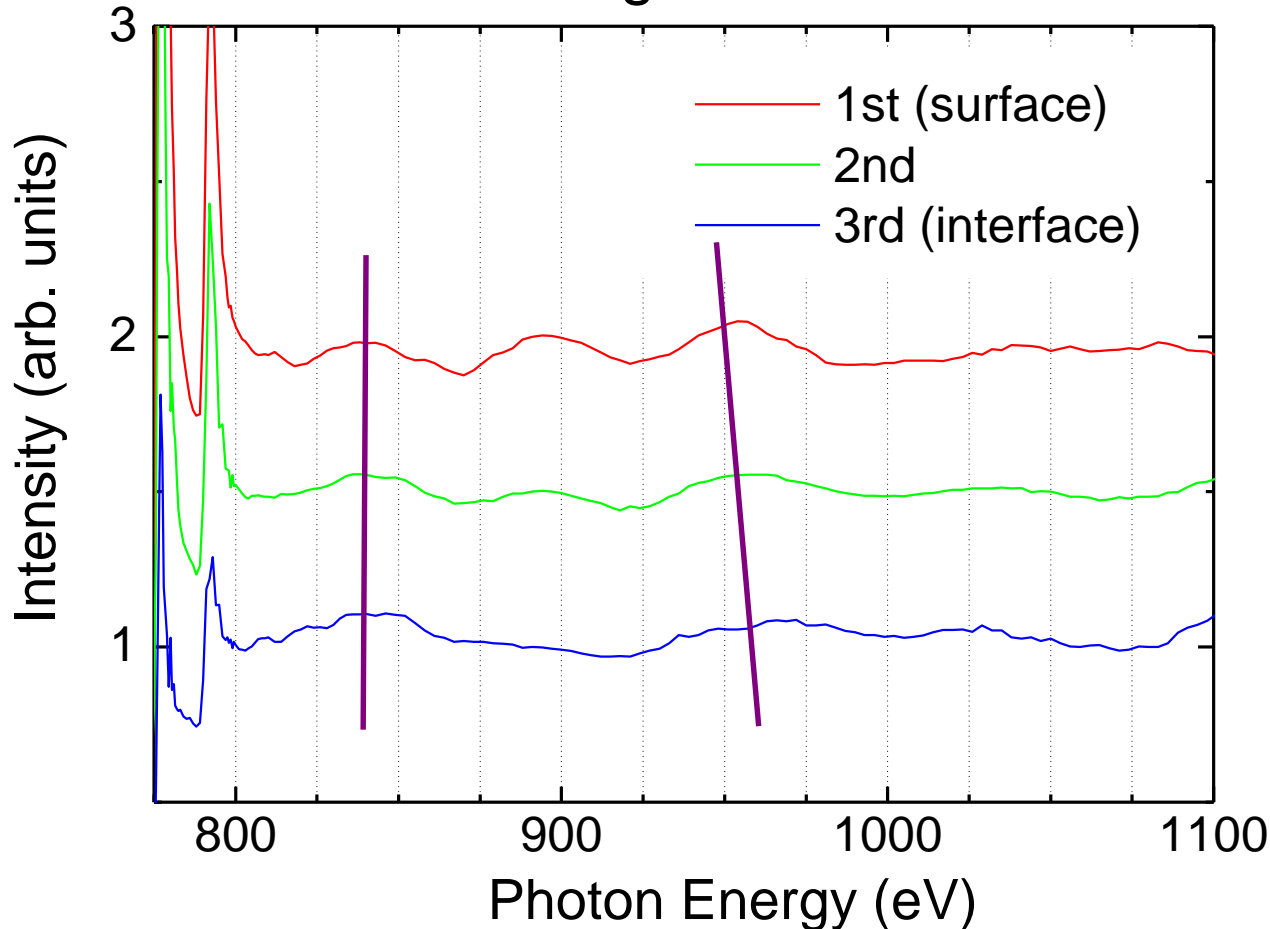
It might be true...

Surface shows longer oscillation period: shorter bond length

Depth-resolved EXAFS at grazing incidence

Longer out-of-plane bond length at surface?

Grazing Incidence

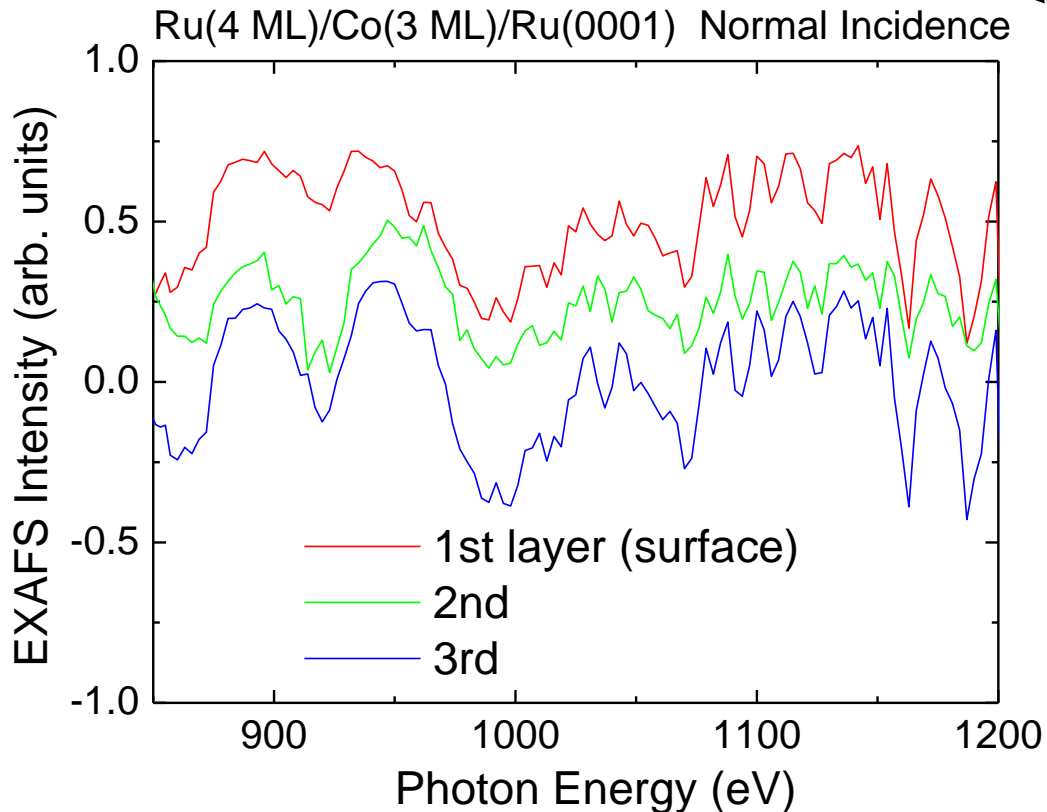


Preliminary analyses

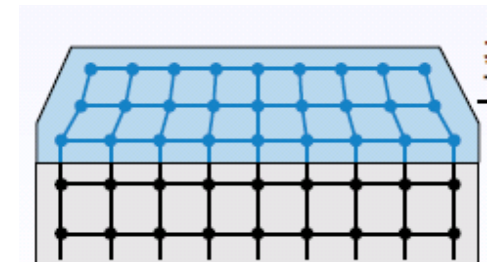
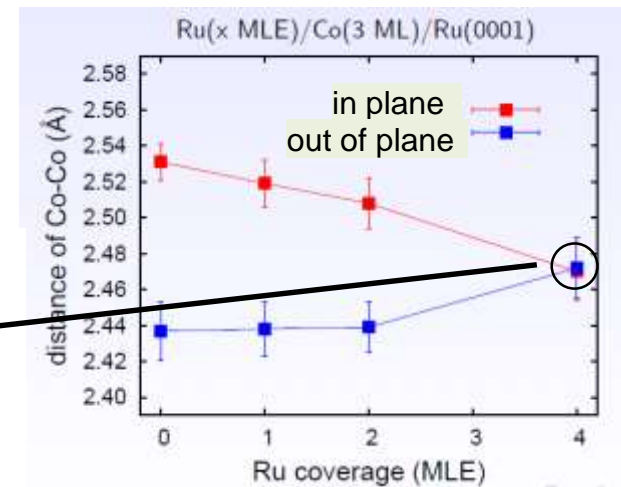
Effects of Ru capping

Normal incidence: in-plane bond length

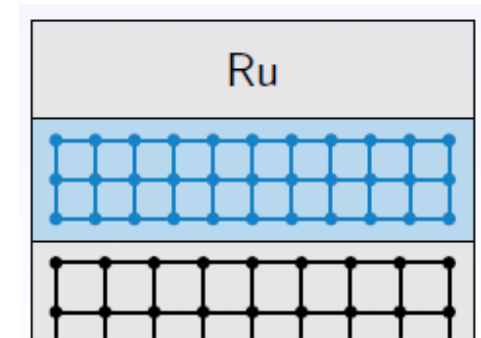
Layer-resolved EXAFS



Little difference in the bond length



↓ Relaxation



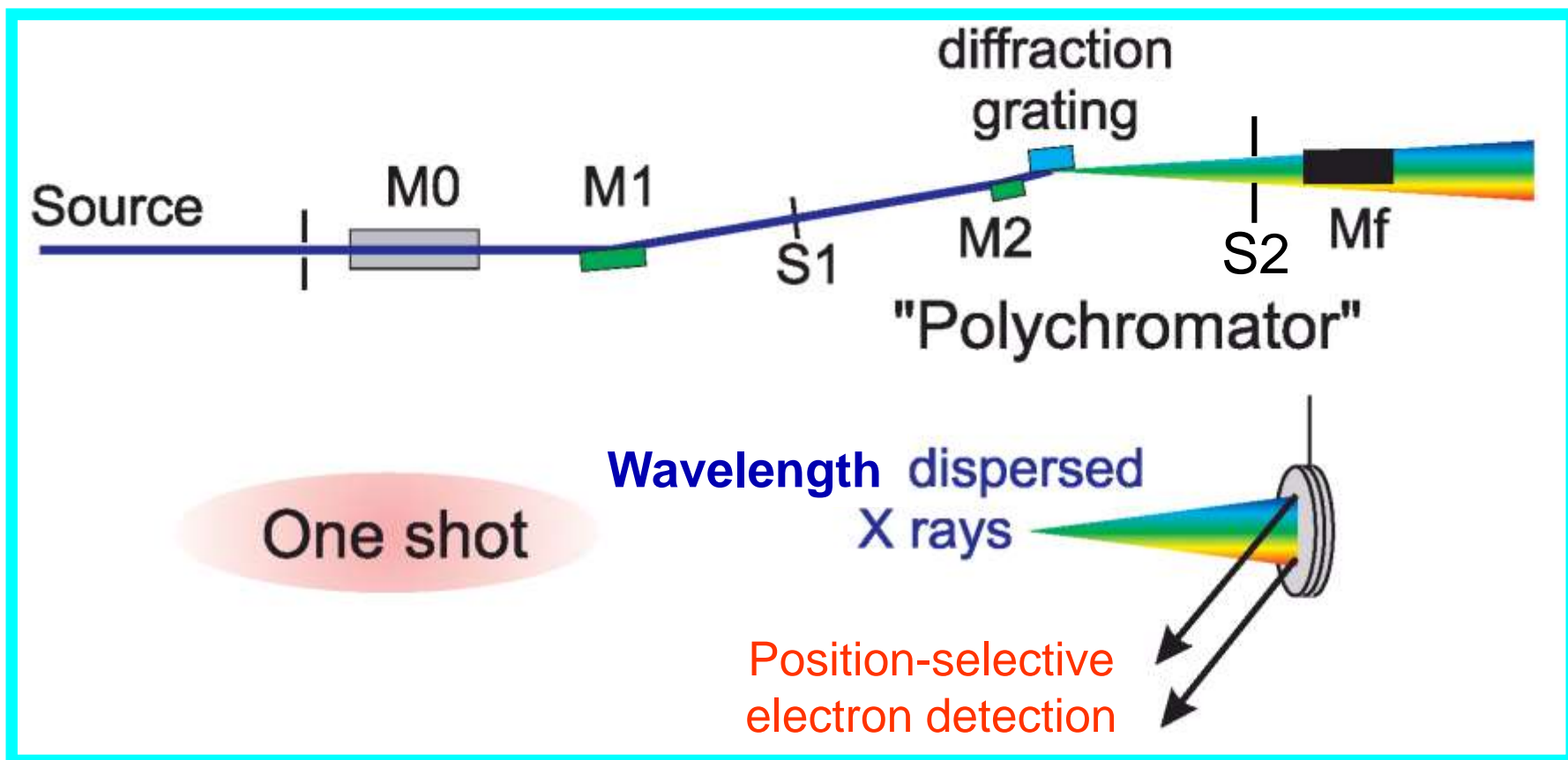
1. Advantages and Disadvantages of
Soft X-ray Absorption Spectroscopy (SXAS)
2. SXAS studies on Surface and Thin films
3. Novel SXAS Techniques
 - 3-1. Depth-resolved XAS
 - 3-2. Wavelength-dispersive XAS

Development of Wavelength-dispersive XAS

XAS: **Element selectivity, Chemical species determination, Structural information,...**

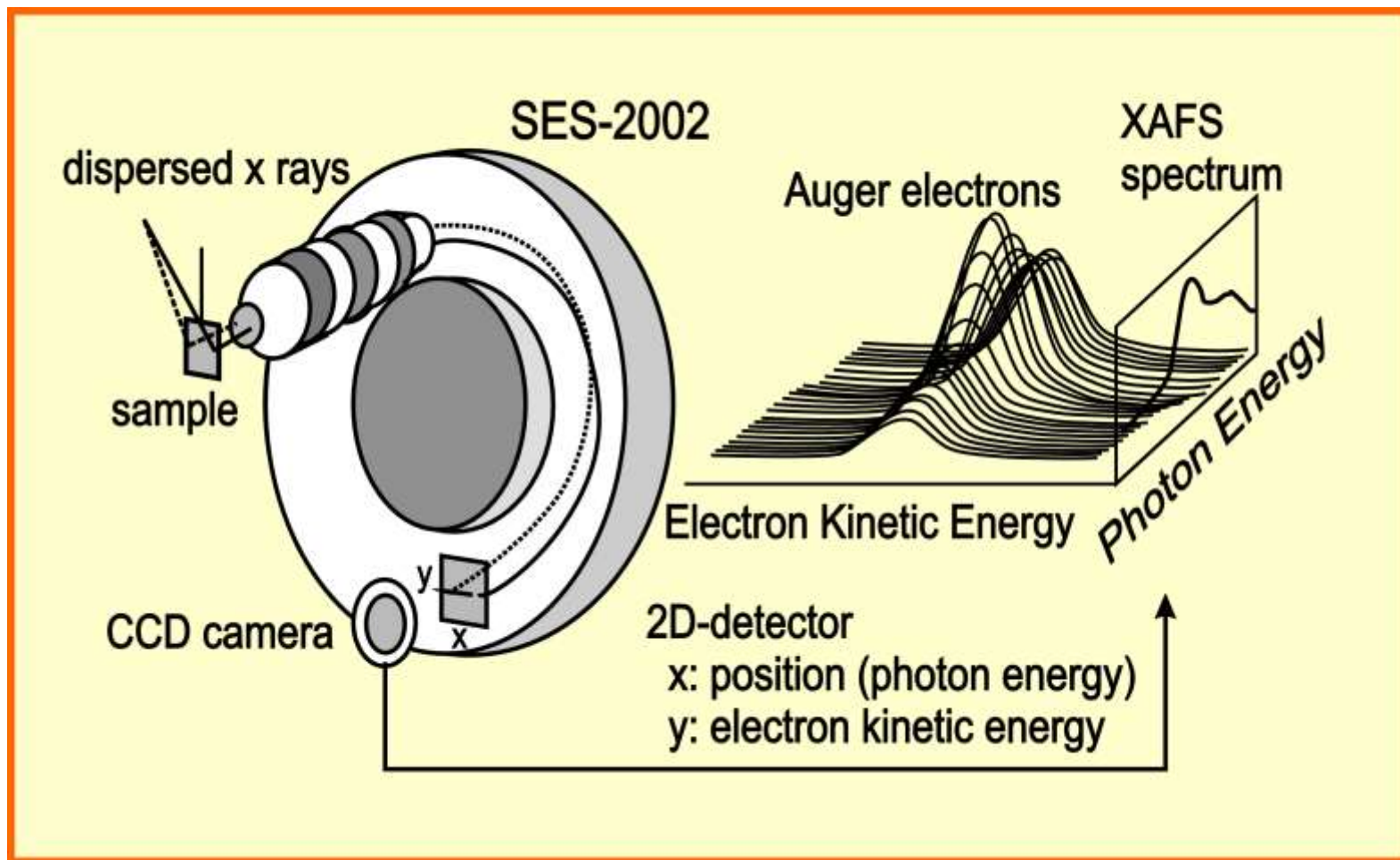
Takes long time (~5 min/spectrum) for a measurement.

Possibility of "One shot" measurement.



Experimental setup for wavelength-dispersive XAS

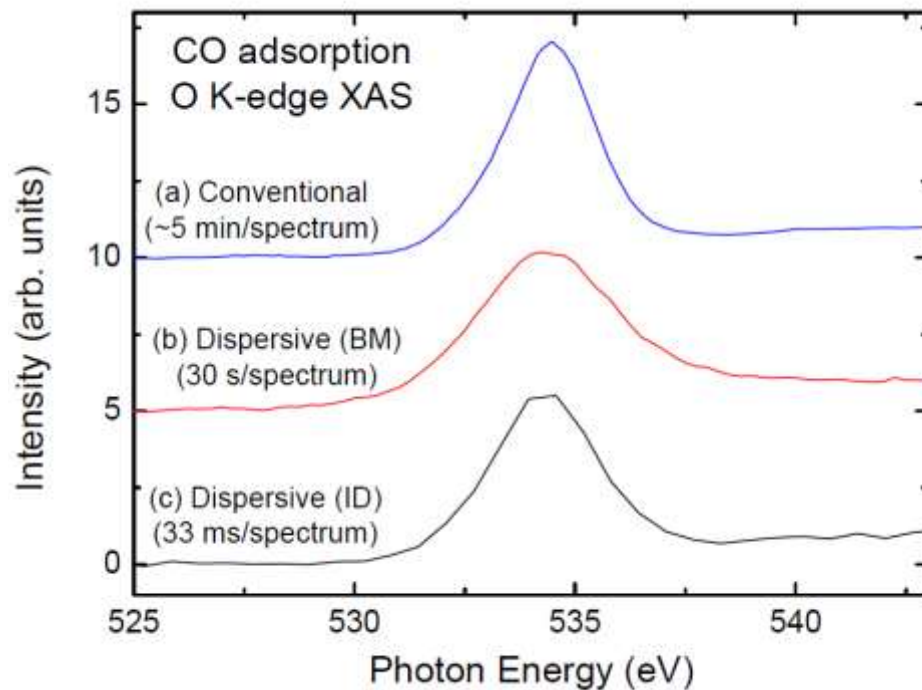
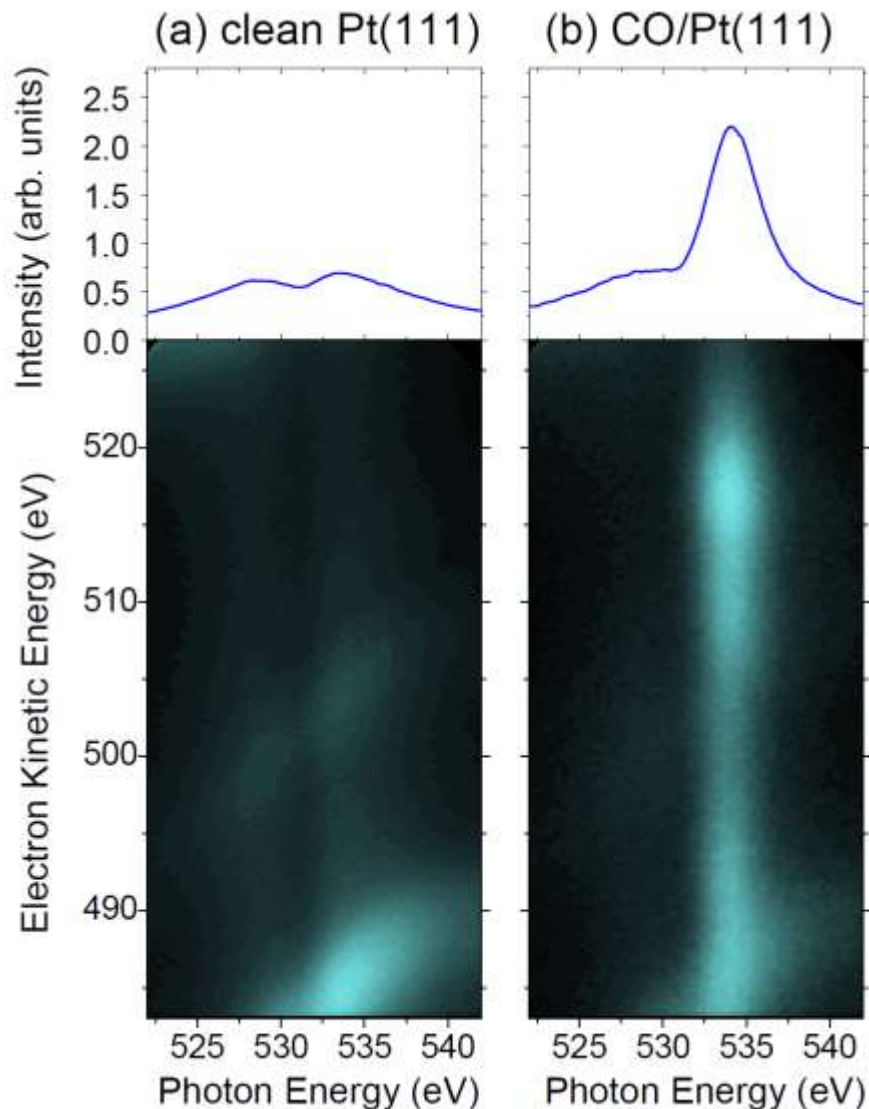
- Wavelength-dispersed X rays + Position-sensitive electron detector



Comparison with conventional XAS

Amemiya et al., Jpn. J. Appl. Phys. **40** (2001) L718.

Amemiya, 放射光, **25** (2012) 269.



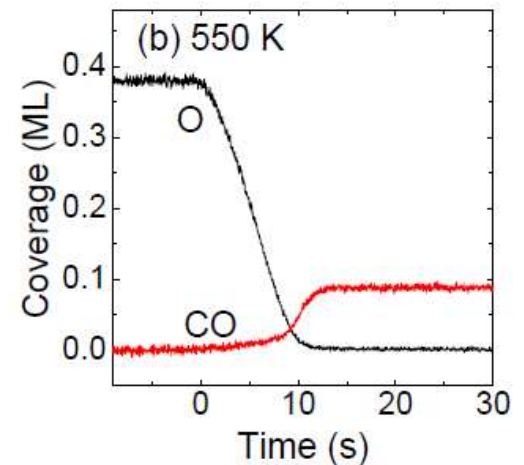
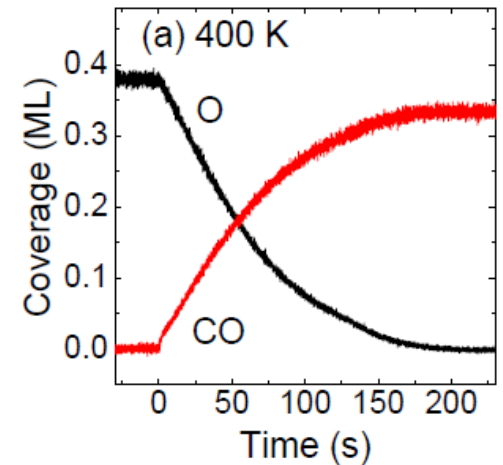
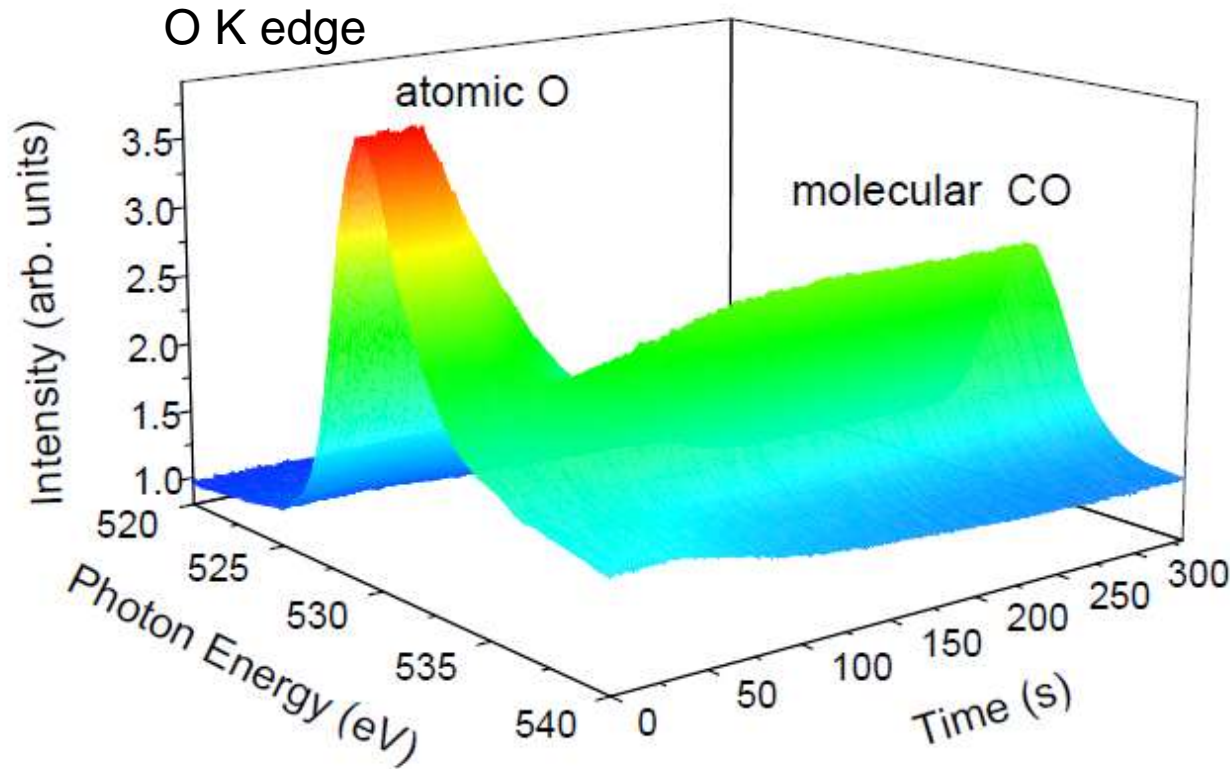
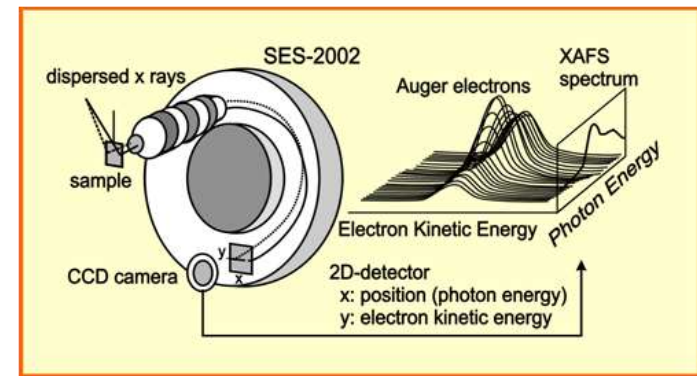
Data acquisition time: 1/10,000 !

Observation of Chemical Reaction

Undulator beamline (BL-16A)

Video rate (30 Hz: 33 ms resolution)

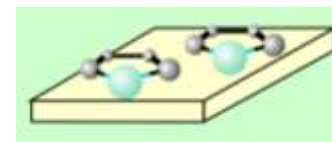
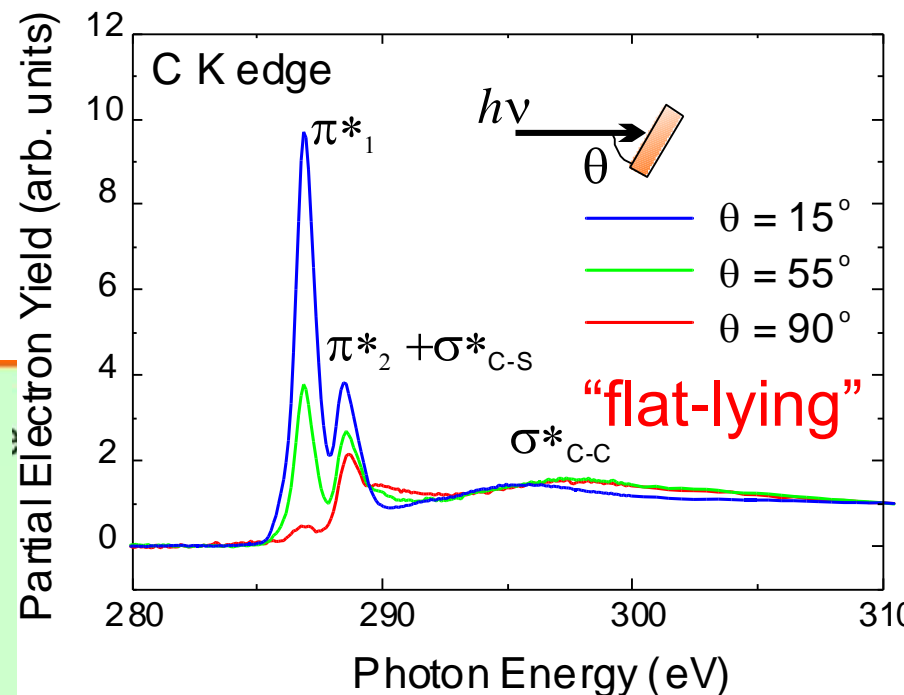
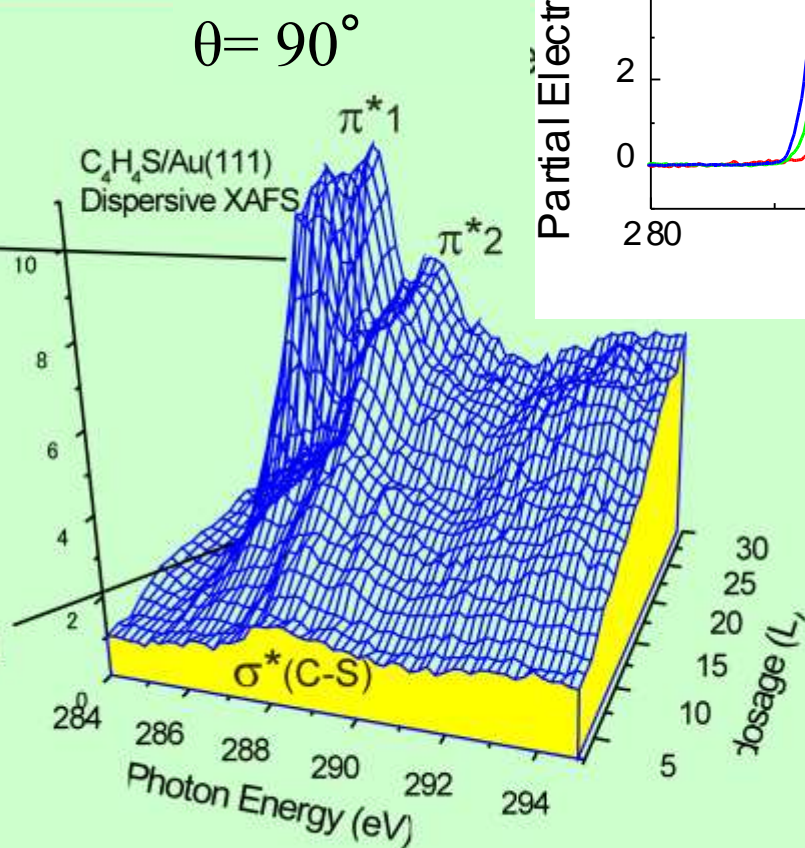
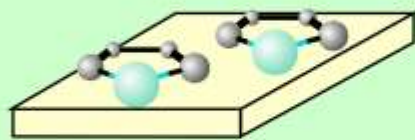
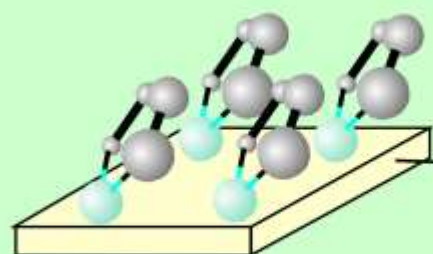
CO + O reaction on Ir(111): $\text{CO} + \text{O} \rightarrow \text{CO}_2 \uparrow$



K.Amemiya et al., Appl. Phys. Lett. **99** (2011) 074104.

Determination of Molecular Orientation

Adsorption of C_4H_4S on Au(111)

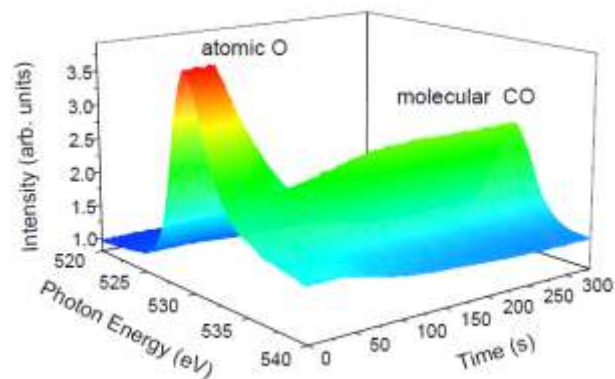


Orientation change
with increasing coverage

Development of Real-time Observation of Orientation

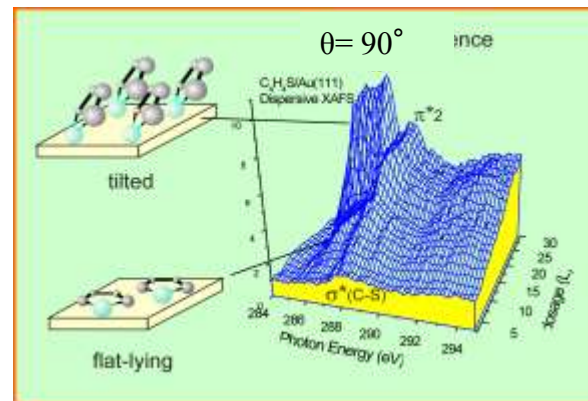
Combination of **dispersive XAFS** and **linear polarization switching** between horizontal and vertical polarizations

Dispersive XAFS



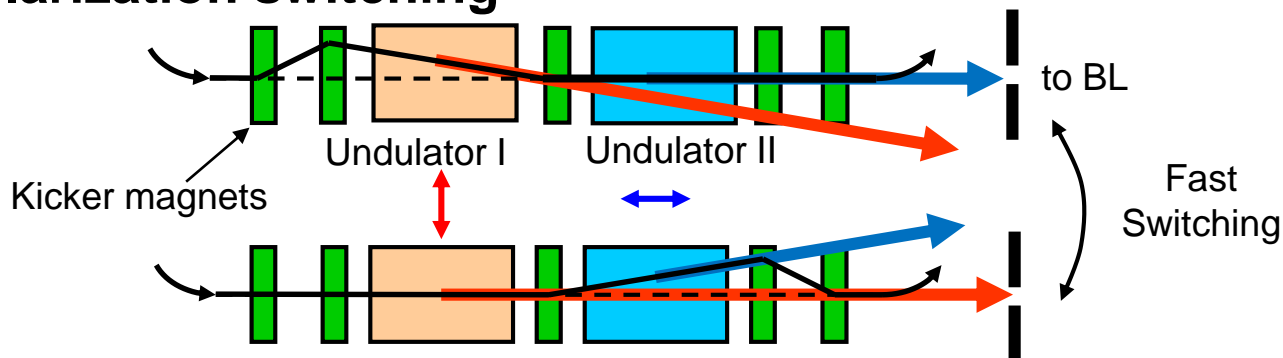
K. Amemiya et al., Appl. Phys. Lett. **99** (2011) 074104.

Polarization dependence



K. Amemiya et al., J. Electron Spectrosc. Relat. Phenom. **124** (2002) 151.

Polarization switching



T. Muro et al., AIP Conf. Proc. **705**, 1051 (2004); **879**, 571 (2007).

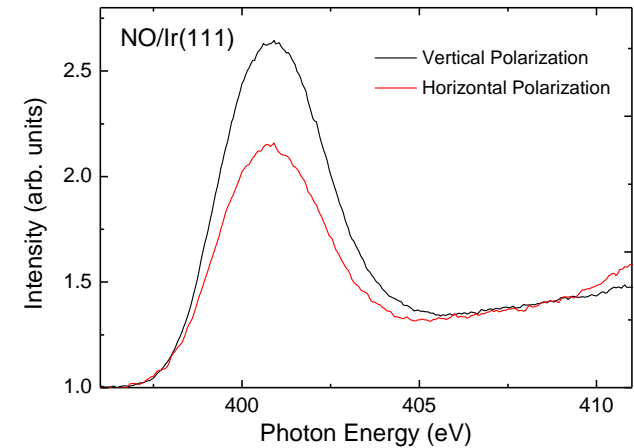
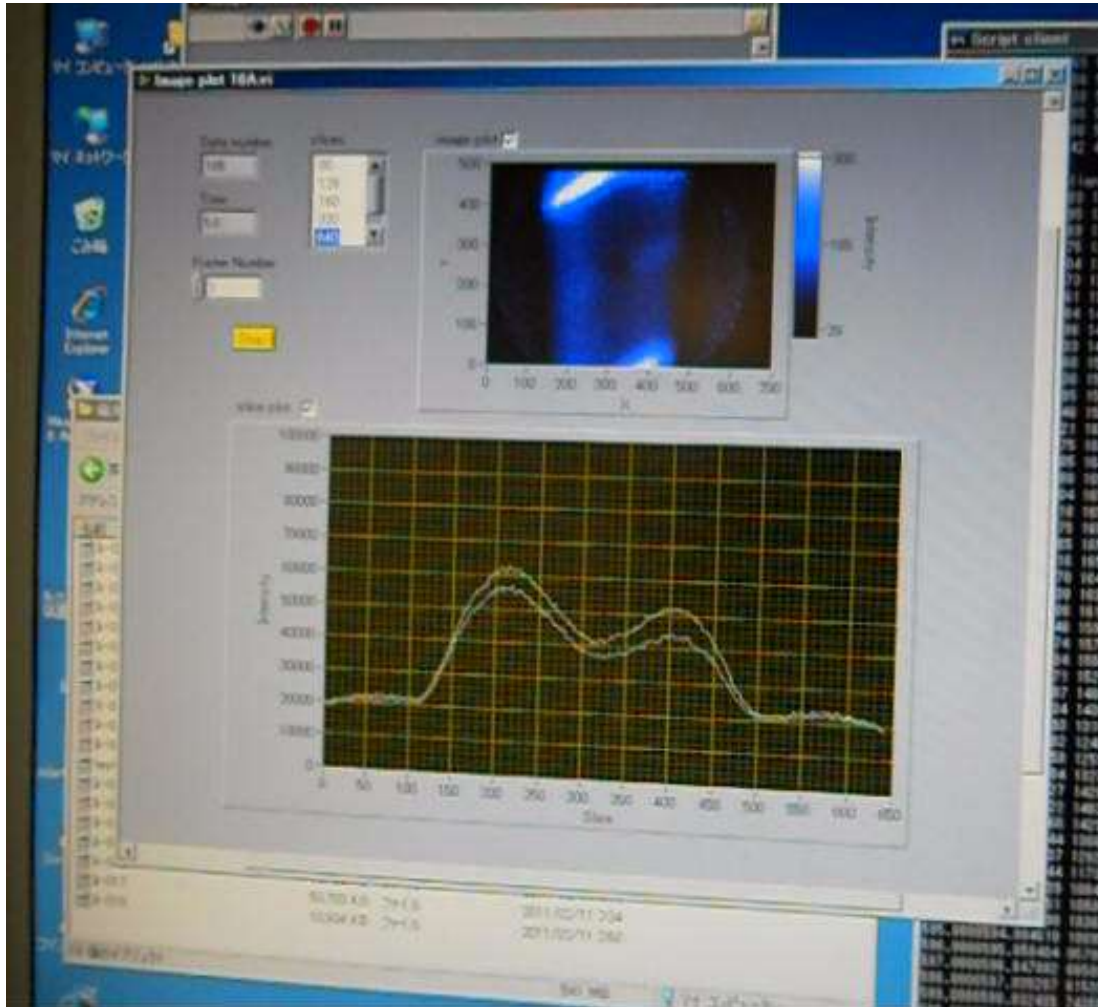
T. Muro et al., J. Electron Spectrosc. Relat. Phenom. **144-147**, 1101 (2005).

K. Amemiya et al., J. Phys.: Conf. Ser. **425**, 152015 (2013).

Combination of Dispersive XAFS and Polarization Switching

Adsorption of NO molecule on Ir(111)

1 Hz switching between horizontal and vertical linear polarizations



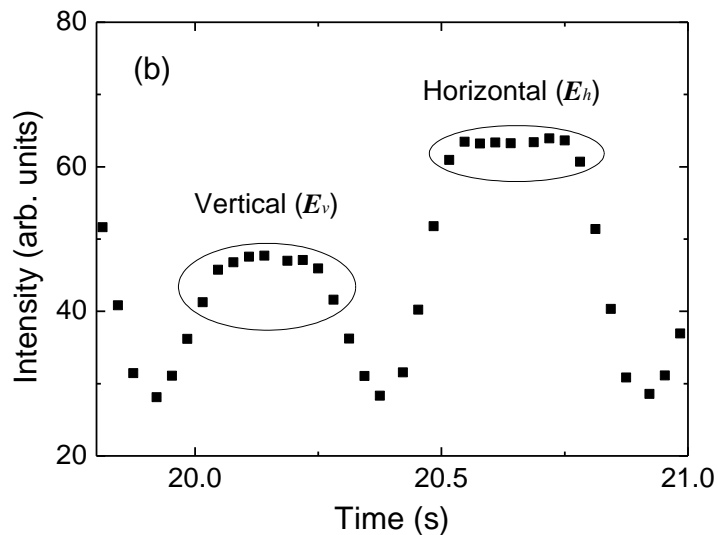
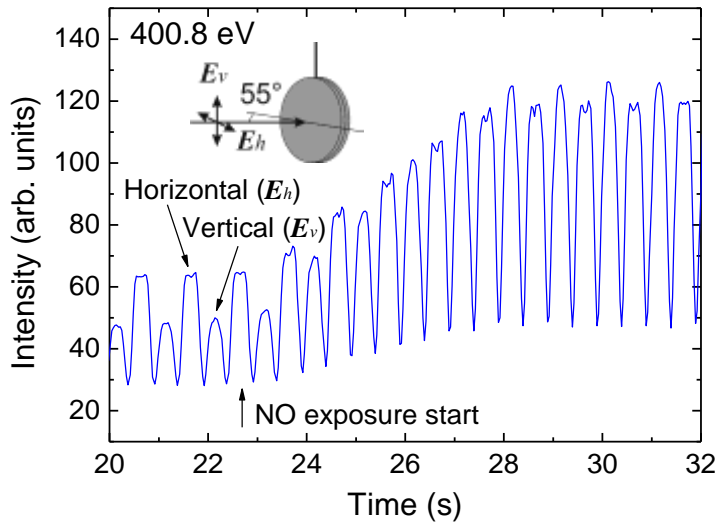
10 Hz switching is now available
(measurement: 1000 Hz)



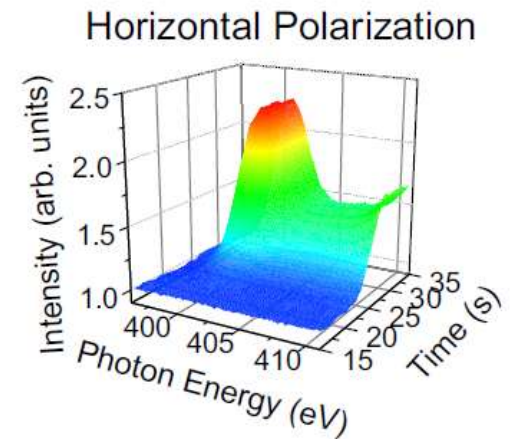
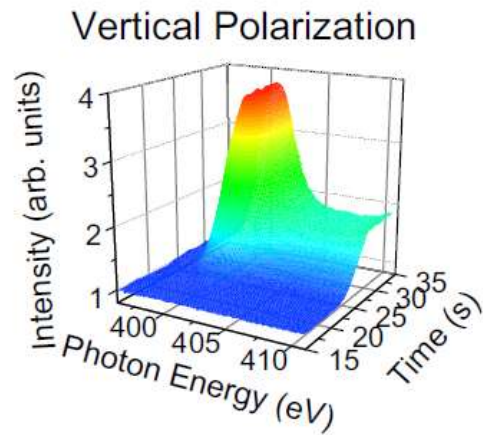
Real-time Observation of Molecular Orientation

Amemiya et al., Appl. Phys. Lett., 101 (2012) 161601.

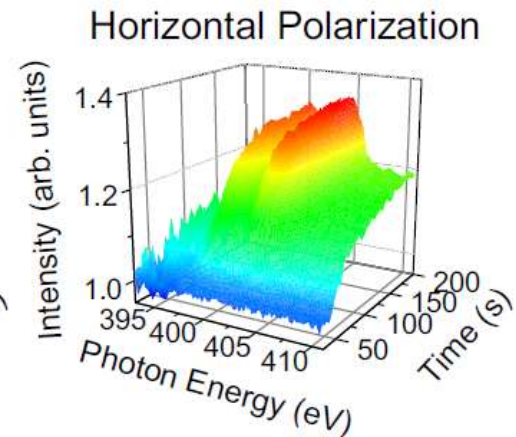
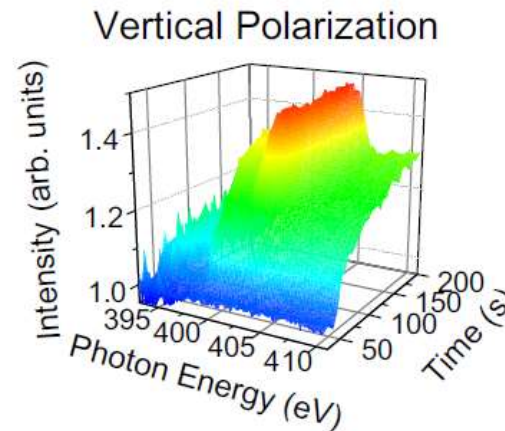
1 Hz switching



(a) NO/Ir(111) N K edge



(b) N₂O/Ir(111)

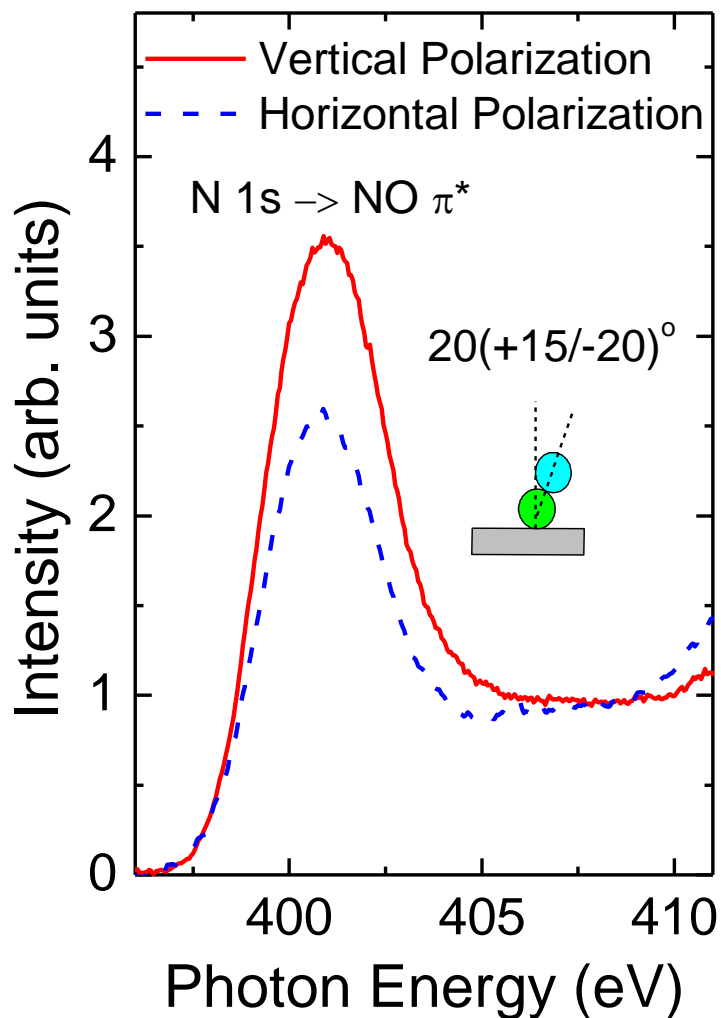


Polarization Dependence at Saturation Coverage

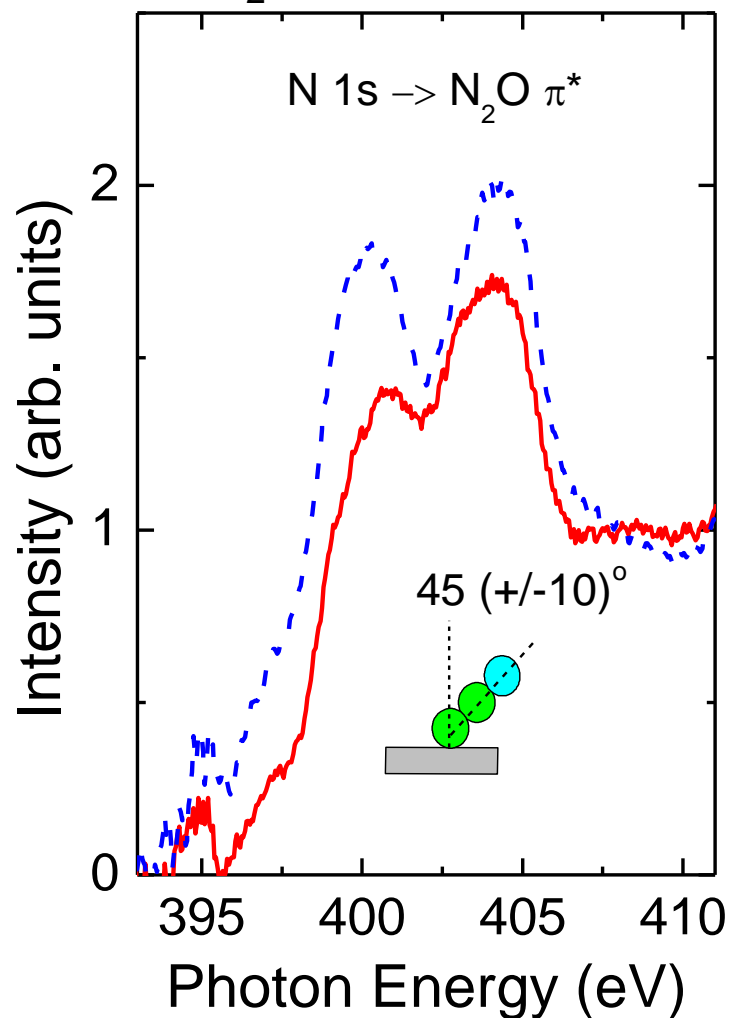
Amemiya et al., Appl. Phys. Lett., 101 (2012) 161601.

N K edge

(a) NO/Ir(111)



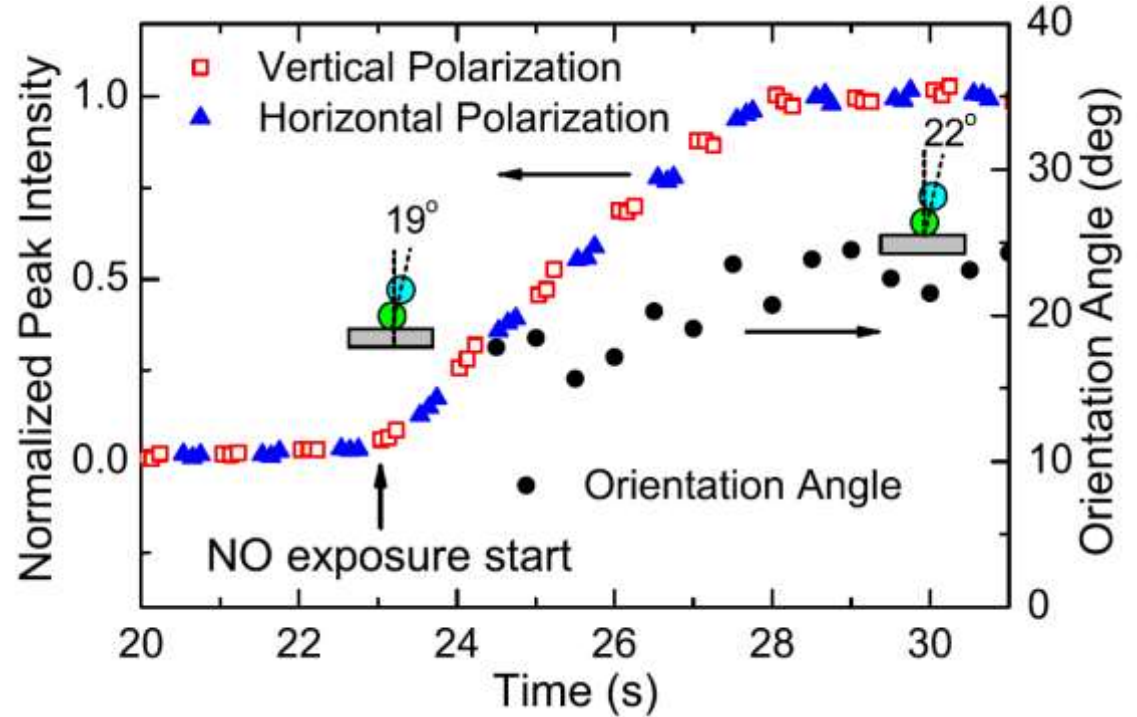
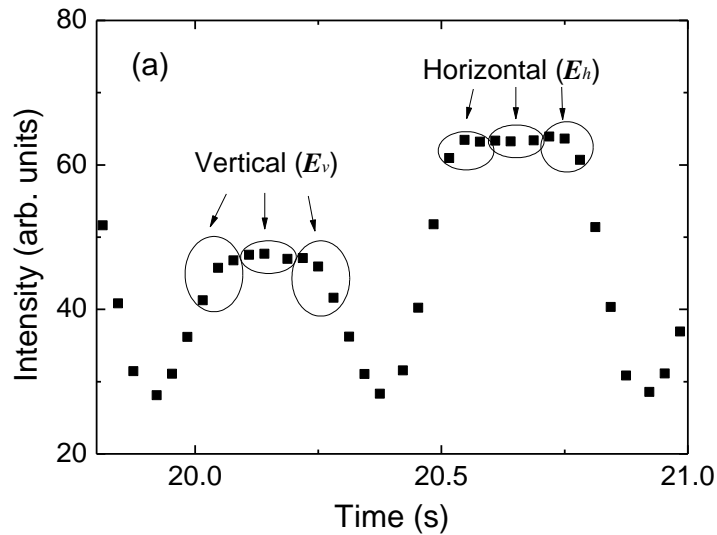
(b) N₂O/Ir(111)



Molecular Orientation Change during NO Adsorption

Amemiya et al., Appl. Phys. Lett., 101 (2012) 161601.

Molecular adsorption of NO at 140 K

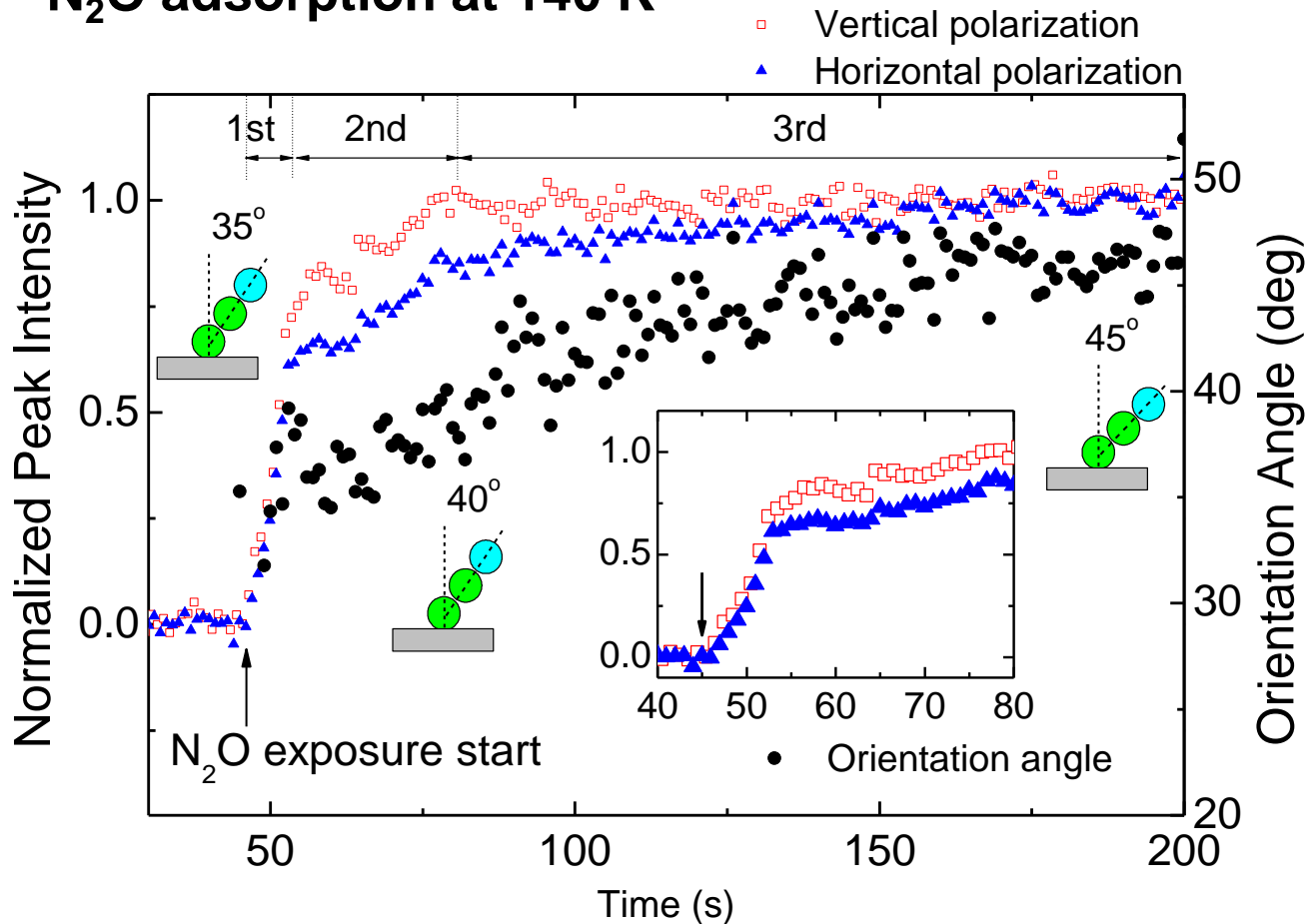


Simultaneous increase between vertical and horizontal polarizations
=> **Constant orientation during adsorption**

Molecular Orientation Change during N₂O Adsorption

Amemiya et al., Appl. Phys. Lett., 101 (2012) 161601.

N₂O adsorption at 140 K



Three stages with different adsorption rates

Averaged orientation gradually increases

1st stage: Fast adsorption up to ~2/3 of saturation. **Constant orientation at ~35°.**

2nd stage: Up to ~90% of saturation. Gradual increase in orientation angle.

⇒ Suggests **another adsorption site** with 45-50° orientation.

3rd stage: Very slow changes towards saturation adsorption state.

Soft X-ray absorption spectroscopy

- Suitable for familiar materials
 - Organic molecules & polymers
 - Magnetic nano-materials
- Surface sensitive
 - a double-edged sword

